DEVELOPMENT OF HIGH ACCURATE EVALUATION SYSTEMS FOR SUGARCANE QUALITY USING COMBINED NON-DESTRUCTIVE ANALYSIS

(非破壊センサーの複合利用によるサトウキビの
高度品質評価システムの開発)

Kittipon Aparatana

2023

DEVELOPMENT OF HIGH ACCURATE EVALUATION SYSTEMS FOR SUGARCANE QUALITY USING COMBINED NON-DESTRUCTIVE ANALYSIS

(非破壊センサーの複合利用によるサトウキビの高度品質評価システムの開発)

By

Kittipon Aparatana

(キッチポン　アーパーラタナ)

This Dissertation Submitted in Partial Fulfillment

of the Requirements for the Degree of

Doctor of Agriculture

Kagoshima University

United Graduate School of Agricultural Sciences

Regional Resource Environment Engineering Course

2023

This dissertation entitled **Development of High Accurate Evaluation System for Sugarcane Quality using Combined Non-Destructive Analysis** hereto attached, prepared, and presented by Kittipon Aparatana in partial fulfillment of the requirements for the degree of Doctor of Philosophy is hereby accepted

Dr. Eizo Taira
Major Advisor

Professor
University of the Ryukyus

Dr. Munehiro Tanaka
Sub Advisor

Professor
Saga University

Dr. Takeshi Shikanai
Sub Advisor

Professor
University of the Ryukyus

Dr. Yoshinori Kamitani
Committee

Associate Professor
Kagoshima University

Dr. Muneshi Mitsuoka
Committee

Associate Professor
University of the Ryukyus

Date: February 28, 2023
The United Graduate School of Agricultural Sciences
Kagoshima University

Abstract

Soluble solids content (Brix) and polarimetric sucrose (Pol) are important indexes for evaluating the quality and maturity of sugarcane, and the development of a measurement method that can be evaluated quickly, accurately, and in a short time is desired. In this study, we developed a sugarcane quality evaluation system that combines using a benchtop visible-near infrared (Vis-NIR) spectrometer, a portable Vis-NIR spectrometer, and an unmanned aerial system (UAS).

As the first step, the sugar content of the squeezed sugarcane juice is measured by the conventional measurement method (Horn's method), and the NIR spectrum is acquired with a benchtop Vis-NIR spectrometer to develop a calibration model. Secondly, we measured the Vis-NIR spectra of sugarcane stalks using a portable Vis-NIR spectrometer. A calibration model for directly estimating the sugar content of stalks from the Vis-NIR spectrum of sugarcane stalks was developed using the calibration model obtained in the first experiment. As the third step, we developed a calibration model for estimating Pol sugar content from UAS images taken from the above sugarcane fields. We developed a model using the Pol obtained by a portable Vis-NIR spectrometer and considered the effect of region of interest (ROI) size on image processing.

In the non-destructive evaluation of a small amount of squeezed liquid using a benchtop Vis-NIR spectrometer, we examined the effect of pre-processing of NIR spectra on the calibration model, SNV processing, and the second derivative processing verified to be the most effective of pre-processing to develop the PLSR calibration model. Furthermore, in developing a Pol calibration model for stalks using a portable Vis-NIR spectrometer, it was suggested that second derivative

processing and multiple regression models are more effective for quantitative analysis than direct use of NIR spectra.

In the third stage, the sugar content estimation experiment from UAS, multispectral images were obtained and calculated to the vegetation index (VI), which was used to estimate the sugar content. The results show that NDVI, $CI_{RedEdge}$, and $SRPI_b$ effectively evaluate the sugar content. As a result of examining the ROI size, the number of small pixels was small, so the information other than leaves was reflected relatively large, and the accuracy of the prediction model will be decreased. Pol estimation by vegetation index showed a high correlation between $SRPI_b$ and NDVI. In particular, the Pol estimation model based on $SRPI_b$ images had the highest correlation, with R^2 of 0.87 and RMSEC of 0.6%. This model shows that Pol is related to nitrogen in sugarcane leaves.

Furthermore, we analyzed the Pol estimation from the image of each band using multiple linear regression analysis. We showed that the NIR band influences the sugar content estimation and the information on water, sugar, chlorophyll, etc., is effective. This study showed that the combined use of optical sensors enabled consistent sugar content evaluation from field to post-harvest.

要旨

可溶性固形分含量　(Brix) と旋光糖度 (Pol　糖度) はサトウキビの品質ならびに成熟度を評価するための重要な指標であり，迅速・正確かつ短時間で評価できる計測手法の開発が望まれている。本研究では卓上型の近赤外分光装置 (Vis-NIR　装置)，ポータブル型の可視-近赤外分光装置 (Vis-NIR　装置)，および無人航空システム　(UAS) を複合的に利用したサトウキビ品質評価システムの開発を行った。

第一の段階として搾汁液の　Pol　糖度を従来計測法 (ホーン法) で測定し，さらに卓上型 Vis-NIR 装置で近赤外スペクトルを取得し，これらのデータを利用して微量サンプルの　Pol　糖度を推定する検量モデルを開発した。次に，第二段階としてポータブル型　Vis-NIR　装置を使用してサトウキビ茎の Vis-NIR　スペクトルを測定した。茎の　Vis-NIR　スペクトルから直接的に茎の糖度を推定する検量モデルを，第一実験で得られた検量モデルを利用して開発した。第三段階として，サトウキビ圃場の上空から撮影した　UAS　画像から　Pol　糖度を推定するための検量モデルを開発した。ここでは，ポータブル型 Vis-NIR 装置で取得した Pol 糖度を活用したモデルを開発し，画像処理では関心領域 (ROI) サイズが与える影響について考察した。

卓上型　Vis-NIR　装置による微量搾汁液の非破壊評価では，NIR　スペクトルの前処理が検量モデルに与える影響を検討し，SNV　処理や　2　次微分処理による前処理が有効であることを検証するとともに，PLSR　による検量モデル

を開発した。モバイル型 Vis-NIR 装置を用いた茎の Pol 糖度検量モデル開発では，近赤外スペクトルを直接用いるよりも 2 次微分処理と重回帰モデルが定量分析に 効果的であることを示唆した。

第三段階の UAS からの糖度推定実験では，マルチスペクトル画像を取得し，これから算出できる植生指数 (VI) による糖度推定を検討した。その結果， NDVI，$CI_{RedEdge}$，および $SRPI_b$ がサトウキビの Brix と Pol 糖度推定に有効であることを示唆した。関心領域サイズを検討した結果，小ピクセル数が少ないため葉以外の情報が相対的に大きく反映され，予測モデルの精度は低下した。 植生指数による Pol 糖度推定は， $SRPI_b$ と NDVI の相関が高くなった。特に $SRPI_b$ 画像に基づく Pol 糖度推定モデルは最も相関が高く， R^2 は 0.87，RMSEC は 0.6%となった。このモデルから Pol 糖度 はサトウキビ葉中の窒素と関連している可能性が示唆された。さらに，各バンドの画像による Pol 糖度推定について，重回帰分析を用いて解析を行い，NIR バンドが最も糖度推定に影響していること，水，糖，クロロフィル等の情報が有効であることを示した。本研究により，光学的センサーの複合利用によって，圃場から収穫後まで一貫した糖度評価が可能であることを示した。

Table of Contents

List of Figures

List of Tables

List of Publications

Main paper I

Aparatana K, Naomasa Y, Sano M, et al. Predicting sugarcane quality using a portable visible near infrared spectrometer and a benchtop near infrared spectrometer. *J near Infrared Spec* 2022; 31:14-23. DOI: 10.1177/09670335221136545.

Main paper II

Aparatana K, Ishikawa D, Maraphum K, et al. Non-destructive Laboratory Analysis of the Detection of Unhealthy Sugarcane Stalks Using a Portable Vis-NIR Spectrometer. *Engineering in Agriculture, Environmental and Food 2022*; 15: 72-80. DOI: 10.37221/eaef.15.2_72

Related paper

Aparatana K, Saengprachatanarug K, Izumikawa Y, et al. Development of sugarcane and trash identification system in sugar production using hyperspectral imaging. *J near Infrared Spec* 2020; 28: 133-139. DOI: 10.1177/0967033520905369.

Acknowledgments

The dissertation titled "The Development of Highly Accurate Evaluation Systems for Sugarcane Quality Using Combined Non-Destructive Analysis" could not have been completed without the invaluable support and guidance of several individuals and organizations.

First and foremost, I would like to express my sincere gratitude to Dr. Eizo Taira, professor at the Laboratory of Agricultural Facilities Engineering, Faculty of Agriculture, The University of the Ryukyus, for his unwavering kindness, generous support, and valuable guidance throughout this study. Dr. Taira's knowledge and expertise were instrumental in solving numerous problems that arose during this research. I am deeply grateful for his encouragement and advice that motivated me to complete this dissertation successfully.

I also extend my heartfelt appreciation to Assoc. Prof. Dr. Muneshi Mitsuoka, lecturer at the same laboratory, for his consistent guidance and insightful advice during this study. My thanks also go to Prof. Dr. Takeshi Shikanai and Prof. Dr. Munehiro Tanaka for their valuable input and encouragement.

I am indebted to the examining committee member for their constructive evaluation and useful suggestions that helped improve this dissertation.

The success of this study would not have been possible without the diligent assistance of Hitoshi Agarie, a researcher at the Laboratory of Agricultural Facilities Engineering, who helped collect data using a drone, and Dr. Kenta Watanabe, a researcher at the Crop Science Laboratory, who provided sugarcane for use in this study. I am also grateful for the support of Kosuke Takahashi and Yumika Naomasa,

graduate students, Morito Sano, an undergraduate student, and Yoshinari Izumikawa, a senior and a close friend, who provided invaluable help in the laboratory.

Furthermore, I would like to acknowledge the financial support of Grant-in-Aid for Japan Society for the Promotion of Science (JSPS) research fellow number JP21J14214 and the National Agriculture and Food Research Organization (on-farm demonstration trials of smart agriculture).

Finally, I cannot overstate the support of my family, whose unwavering belief in me kept me motivated throughout this long-term study in Japan. I would also like to express my gratitude to all those who may not have been mentioned but have contributed to the success of this study.

Kittipon Aparatana

Chapter 1: Introduction

This chapter provides an overview of the study, starting with the background (section 1.1) and contextual information (section 1.2), followed by the specific aims and objectives of the research (section 1.3). Additionally, section 1.4 outlines the significance and scope of the study and includes definitions of key terms used throughout the text. Finally, section 1.5 discusses the anticipated benefits of the research.

1.1 BACKGROUND

Sugarcane (*Saccharum officinarum* L.) is a high-biomass-yielding crop containing a large amount of sugar. Thus, it is mainly used for sugar and biofuel production[1]. In Japan, sugarcane is mostly grown on southern islands at 24–31N latitude and 123–131E longitude. A total of 16 raw-sugar mills are scattered across these islands. Although sugarcane production in Japan is relatively small, accounting for less than 0.1% of the world's production, sugarcane is one of the most important agricultural products supporting the local economy. Sugarcane quality and yield are two of the most important indices for millers and producers because the cane price is determined based on the sugarcane quality.

In contrast, the yield determines the total output. The primary criteria for measuring the sugar quality are polarimetric sucrose (Pol), total soluble solids (Brix), and the purity coefficient of sugarcane where the conventional method[2] is a method to measure the Pol and Brix in sugar mills (Figure 1.1). However, this method is time-consuming and requires considerable skill and care to obtain sufficient

sugarcane juice needed for the measurements (Figure 1.2). Brix is used to determine the approximate quantity of sugar present in agricultural products. It can be measured from a small amount of juice using a refractometer (Figure 1.3). Brix is commonly used as a sugar index for the samples. However, sugarcane juice also contains other components besides sugar, which are unnecessary in the valuation of sugarcane, such as minerals and reducing sugar. Pol is determined by Brix and Pol readings (International Sugar Scale). Pol readings are measured from 100 mL of clear cane juice using a polarimeter (Figure 1.4). However, obtaining clear juice involves squeezing, clarification with a toxic chemical, and filtration, which creates hazardous waste. The purity coefficient is calculated from %Pol divided by %Brix, which serves as a maturity index that can be used to determine the best harvest time. Although these quality indices (i.e., Pol, Brix, and purity) are important for farmers and millers before the harvest, a measurement method that can be used in the farmland has not yet been developed.

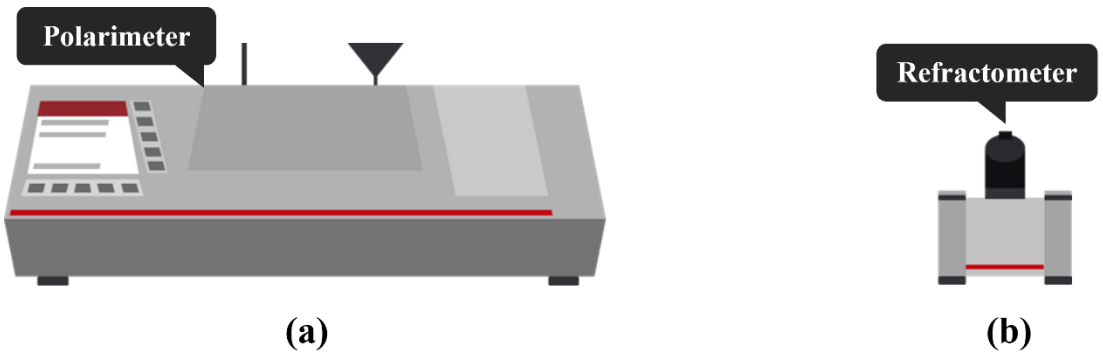

Figure 1.1: The conventional method contains two instruments; (a) a polarimeter and (b) a refractometer

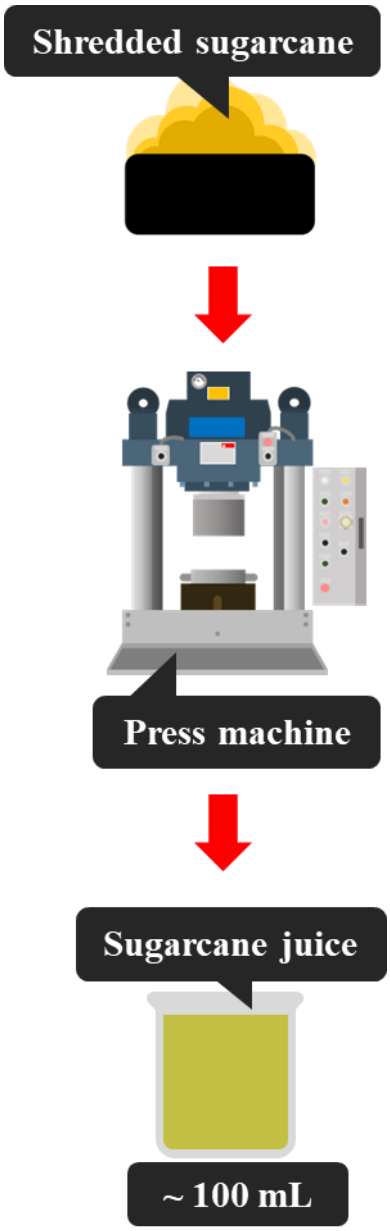

Figure 1.2: Diagram of process to obtain sugarcane juice in sugar mill using press machine

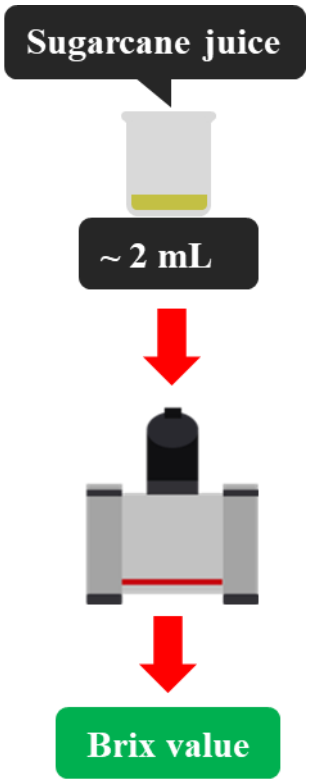

Figure 1.3: Diagram of present process to obtain sugarcane Brix value in sugar mill

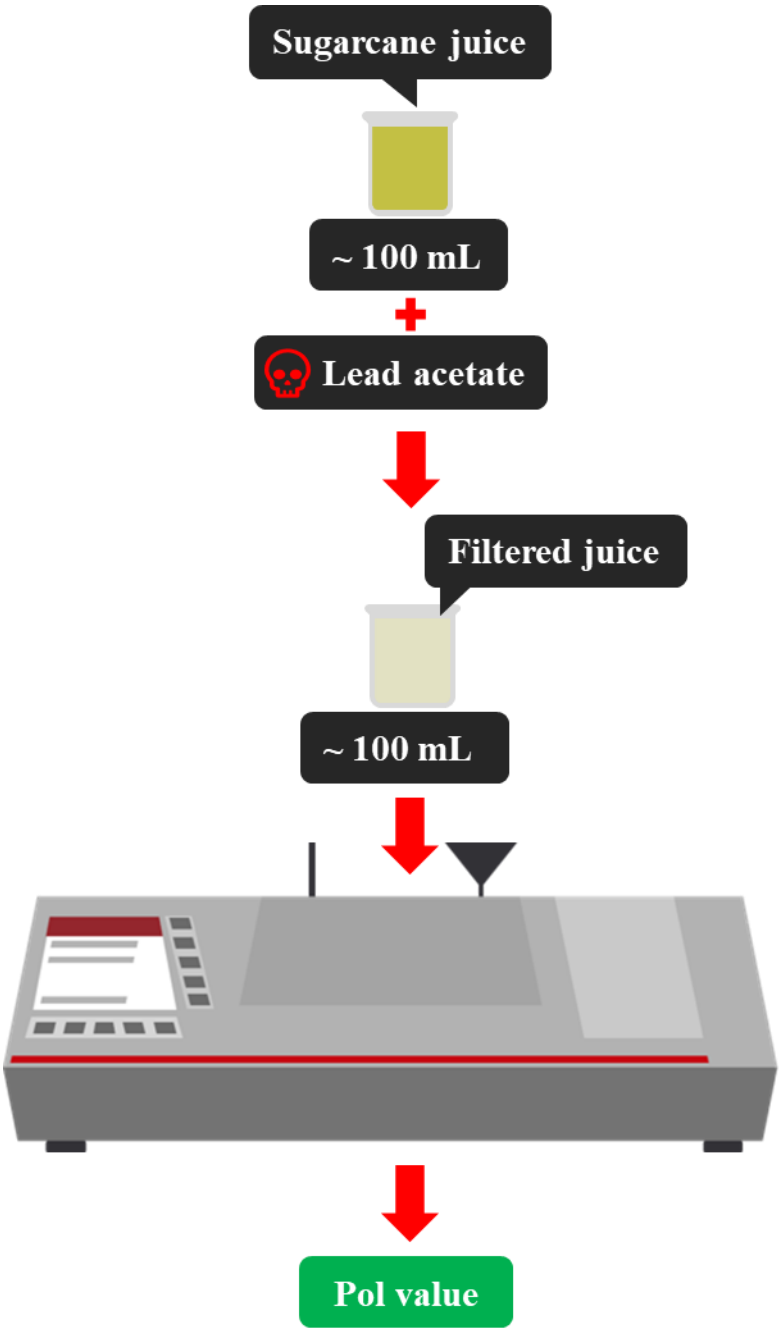

Figure 1.4: Diagram of present process to obtain sugarcane Pol value in sugar mill

Spectroscopy is a rapid and accurate technique used in many agricultural applications. This method involves the analysis of interactions of light with matter, which is achieved by measuring changes in the wavelengths of light as parts of it get absorbed by the molecular moieties of the studied materials. For example, in the case of food and forage materials, molecular moieties containing C–H, N–H, and O–H

bonds show absorption bands within 1400–2500 nm, which correspond to the biological signatures of materials such as water and sugar content[3]. Because of these advantages, NIR spectroscopy is used to perform sugarcane quality measurements. A near-infrared (NIR) spectrum can be acquired in less than a minute. As shown in Figure 1.6, The sugar quality estimated through calibration using the NIR spectrum of shredded cane corresponds to that measured by the slower, conventional method. Therefore, benchtop Vis-NIR spectrometers have been introduced in all Japanese sugar mills, and the current quality-based payment system has been employed since the 2005/2006 harvest season. The data can be shared on the network system. This data can later be combined with that obtained by other mills of different regions to further improve the accuracy of the calibration model[4]. However, benchtop Vis-NIR spectrometers are not mobile and require of shredded cane which need to be shredding with sugarcane cutter glider (Figure 1.7). Therefore, measurement methods that can be used in the farmland still need to be developed.

Figure 1.5: Diagram of using benchtop Vis-NIR spectrometer in sugar mill

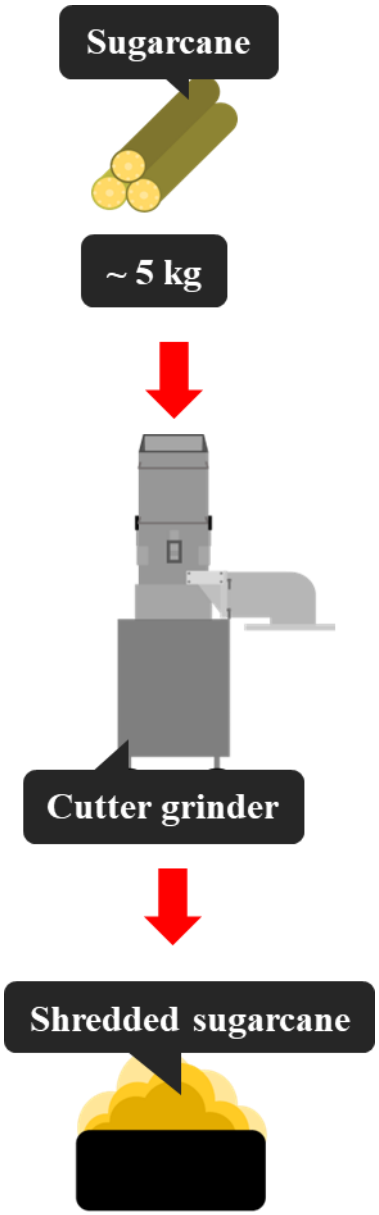

Figure 1.6: Diagram of process to obtain shredded sugarcane in sugar mill using cutter grinder

The abovementioned problems can be resolved using a portable visible-NIR (Vis-NIR) spectrometer (Figure 1.7). A Vis-NIR spectrometer can be used in the laboratory or the field by aiming its emitter beam directly onto the surface of the selected internode of a sugarcane stalk (Figure 1.8). Thereafter, the spectral information (400-1000 nm) for predicting the sugar quality can be collected within

approximately 10 s without damaging the sugarcane plant[5-7]. Furthermore, the method may be more accurate than the refractometer as the Vis-NIR beam covers the whole internode. This fast, easy, and non-destructive measurement system is expected to be quite useful; therefore, a good calibration model should be developed for its practical application.

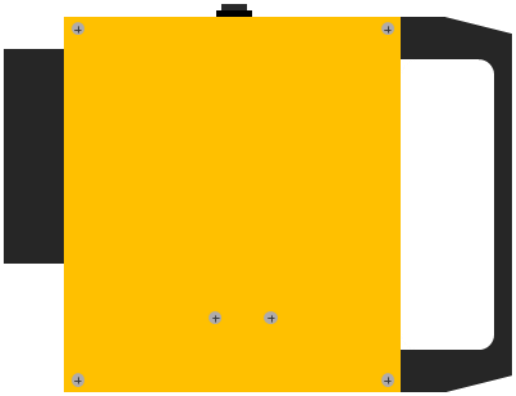

Figure 1.7: A portable Vis-NIR spectrometer

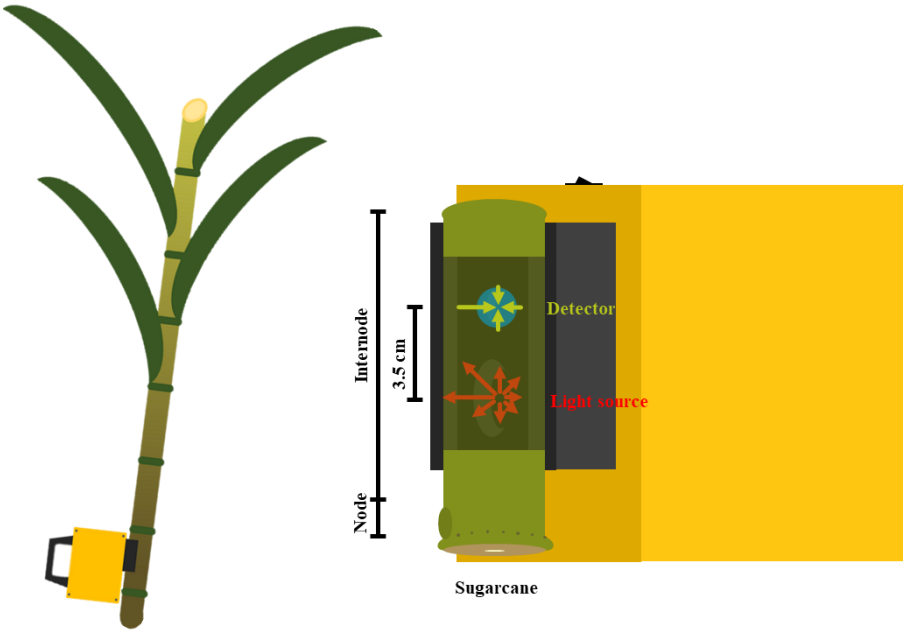

Figure 1.8: Example of demonstration of using a portable Vis-NIR spectrometer

The chlorophyll, water, and sugar bands were the key to developing the sugar quality prediction model for a portable Vis-NIR spectrometer. Chlorophyll plays an important role in the visible range because it is the most common pigment in plants and is involved in photosynthesis which is considered related to sugar quality in the case of sugarcane. Chlorophyll helps absorb energy from sunlight and converts light energy into chemical energy. Chlorophyll appears green because it absorbs light well at a wavelength of approximately 400–500 nm and 600–700 nm – i.e., blue and red-reflecting green light. Another photosynthetic pigment, called carotenoid, absorbs light energy but passes it to the chlorophyll molecules. Chlorophylls are blue-green (chlorophyll–a) or green (chlorophyll– b) in color, whereas carotenoids are orange (carotenes) or yellow (xanthophyll). Analyzing chlorophyll in sugarcane using leaves canopy reflectance images might lead to assessing the sugarcane vegetation state and sugar quality.

A multispectral camera mounted on a small unmanned aerial system (UAS) is the new instrument for future yield and sugar quality estimation[8] (Figure 1.9). For example, a multispectral camera mounted on a small UAS could collect mass information of sugarcane canopy reflectance information and solve the problem of row obstacles in the sugarcane field that a portable Vis-NIR spectrometer could not access. Vegetation indices (VIs) are simple spectral imaging that combines two or more image bands to enhance the vegetation properties in the image. VIs are sensitive to leaf changes and are helpful for estimation research[9]. For example, the Normalized difference vegetation index (NDVI) is sensitive to the leaves area of the plant, the Chlorophyll index red edge ($CI_{RedEdge}$) is sensitive to chlorophyll in leaves, and The Simple ratio pigment index ($SRPI_b$) is sensitive to nitrogen in leaves[10]. This phenomenon is related to the photosynthesis of the sugarcane cycle and might be

directly or indirectly sensitive to the change in sugarcane maturity, health, and sugar quality[11]. However, a complete field image requires expensive software to generate and combine the map, and it takes time before calculating the vegetation indices and further analysis.

Figure 1.9: UAS

Nevertheless, developing Pol prediction requires harvesting the sugarcane stalk and bringing it to the laboratory to measure it. Unfortunately, this process permanently damages the sugarcane and takes time to develop the Pol prediction model. Smart agriculture techniques like using a portable Vis-NIR spectrometer on the ground for Pol measurement and capturing the sugarcane canopy reflectance images using a UAS to develop a Pol prediction model might compensate for each instrument's weakness. In addition, this technique might be cost-efficient and faster.

1.2 CONTEXT

The sugar mill needs to improve the use of benchtop Vis-NIR spectrometer and find a new tools or methods that function faster, non-destructive, and mobile to predict sugar quality at both field and laboratory.

1.3 PURPOSES

The study aim was (I) to develop a sugarcane quality calibration model for the benchtop Vis-NIR spectrometer using sugarcane juice spectral analysis results and sugarcane quality as measured by the conventional method, (II) to develop a sugar quality calibration model for a portable Vis-NIR spectrometer using stalk spectra and the sugar quality predicted from sugarcane juice using the benchtop Vis-NIR spectrometer, and (III) to develop a sugarcane quality calibration model for a multispectral camera mounted on UAS using various cropped sizes of sugarcane reflectance canopy at the region of interest images and sugarcane quality as measured by a portable Vis-NIR spectrometer.

1.4 SCOPE OF RESEARCH

This research was conducted in Okinawa prefecture, Japan, to develop highly accurate evaluation systems for sugarcane quality using popular Japanese cultivars such as Ni27, NiH25, Ni21, NiF8, etc., delivered from 16 sugar industries around Japan. The sugarcane spectra and sugar quality were measured by a polarimeter, refractometer, benchtop Vis-NIR spectrometer, portable Vis-NIR spectrometer, and UAS to analyze and develop calibration models.

1.5 EXPECTED BENEFIT

Author demand to use the benefit of how basic, rapid, and non-destructive a portable Vis-NIR spectrometer is to measure the sugar quality in the field to know when sugarcane has the highest sugar quality or sugarcane maturity stage for future research, where generally previous methods cannot be used like this and most importantly a stalk spectra that measured by a portable Vis-NIR spectrometer could

be used learn more about sugarcane like health, habit, water stress, factors that made sugarcane change in sugar quality, etc. Measure sugar quality in the field monthly using a portable Vis-NIR spectrometer and capturing multispectral image reflectance of sugarcane leaves using UAS might lead to finding a correlation between these data might be a direct or indirect correlation, which will be able to create a sugar quality map, sugarcane maturity map, health map, etc., and will be very useful for both the sugar industry and farmers.

Figure 1.10: Visual imagination of expected benefit

Chapter 2: Literature Review

The literature review chapter serves as the foundation for this study, providing a comprehensive understanding of the subject matter and supporting the research focus. The primary aim of the literature review chapter is to explore the existing theoretical concepts and research findings in order to develop a conceptual framework that can generate hypotheses and address the research problem. The literature review chapter includes a discussion of sugarcane (section 2.1), sugar processing (section 2.2), the use of Near-infrared spectroscopy in sugarcane (section 2.3), spectral correction and pre-treatment techniques (section 2.4), the use of multispectral images and vegetation indices (section 2.5), multivariate analysis (section 2.6), and an overview of related studies (section 2.7).

2.1 SUGARCANE

Sugarcane is a member of the grass family that is known for its high production of sugar. It serves as a vital source of food, renewable energy, and income for millions of people worldwide, occupying over 20 million hectares of land[1]. Typically grown in warm-temperature, tropical, or sub-tropical regions, sugarcane is native to South Asia, Southeast Asia, New Guinea, and South America. At the ripening stage, sugarcane can reach a height of 2-6 meters, with a stalk diameter of approximately 30-60 mm. Historically, people would chew or suck on sugarcane for its natural sweetness, but over time, techniques were developed to extract sugar from the plant. Today, sugarcane agriculture is primarily driven by global demand for sugar.

Sugarcane agriculture is a crucial economic activity in more than 100 countries, especially in developing economies where poverty and unemployment are prevalent. By providing income and employment, sugarcane-based agriculture plays a vital role in the economic growth of these countries, particularly in uplifting under-skilled rural populations. The industry not only supports farmers and laborers but also provides opportunities for related businesses such as transport, storage, and processing. With its ability to generate economic opportunities and contribute to poverty reduction, sugarcane-based agriculture is a significant contributor to sustainable development in many developing economies.

In Japan, sugarcane (Figure 2.1) is an economically significant crop in the southern region[12] because most of the local people are working in the sugar industry for the main work since the increasing of sugarcane production in 2015 along with increasing of the human population. In recent several-year, sugarcane roles in Japan are starting to change after the worker ageing and becomes rarer, which were contrary to the demand for sugar production in the daily of the sugar industry. Sugarcane is a long-term crop that requires a growth period of approximately 10-18 months per harvest[13] and was mostly grown around March and harvested around January on a small island located on the south subtropical island arc of Japan called “Nansei Island”. Growing sugarcane on Nansei island is difficult due to the season of tropical cyclones called “Typhoon", which damages the sugarcane, make weakening, and makes sugarcane fall into the soil. Vulnerable cane can be easier to infect by several diseases and invade by pests that lead to abnormal physiological processes that disrupt its structure, growth, functions, and other activities. Furthermore, unhealthy or infected sugarcane can infect nearby crops, which adversely affects farmers and sugar factories. The diseases in sugarcane are caused mostly by

pathogenic organisms such as fungi, bacteriam, mycoplasma, viruses, viroids, and nematodes.[14, 15] Red-rot is one of the most commonly observed diseases in sugarcane which is caused by the fungus, *Colletotrichum falcatum* Went recently known as *Glomerella tucumanesis* Speg.[14-16] Red-rot can cause a significant loss in the yield as it is difficult to detect in the field through non-destructive testing or through the naked eye. New tools and faster and more accurate methods are crucial in predicting the quality of sugarcane in the field. Extensive research has been conducted to identify unhealthy conditions in sugarcane, including the diagnosis by an expert system application[17], identification using image processing[18], and use of sequence-characterized amplified region (SCAR) markers[19]. In 2022, a portable Vis-NIR spectrometer can also detected unhealthy in sugarcane stalk without damage the sugarcane.

These circumstances make sugarcane difficult to reach the maximum yield of growing and lowers the quality of sugarcane. As a result, around 40 sugarcane cultivars have been developed, and approximately 10 popular cultivars are currently used. One of the most popular is Ni27[20], as shown in Figure 2.2.

Figure 2.1: Sugarcane field in Minami-Daito, Okinawa, Japan

Figure 2.2: Japanese sugarcane (cultivar Ni27)

In the past, sugarcane generally was harvested by labour with a cutting tool (sugarcane knife). Harvesting by labours required a lot of labours and time to harvest in one area[21]. Moreover, some sugarcane cultivars with hairy stalks are caused a

problem in harvesting by resistance to a cutter. This problem makes labour chose to burnt sugarcane before harvest to make it more accessible to cut by labour but burnt cane can produce low payloads and increased losses in the field.

Currently, the burnt cane was reduced by used mechanical harvesting (sugarcane harvester). Sugarcane harvester was performed for harvesting for in a big area, cost-efficiency for labour, and time-efficient, but depends on areas, geography, climates, weathers, labour condition, etc. which are the factors of causing the losses of sugarcane yield in a field. Sugarcane harvesters have 3 major types; harvester equip on tractor, small size harvester, and large size harvester[22]. (Figure 2.3)

Figure 2.3: The sugarcane harvester small type (left) and large type (right)

During the sugarcane harvesting, most of the sugarcane trash are separate with sugarcane harvester de-trashing mechanism, and ditch on the sugarcane field. Then, the sugarcane billet with the rest of the trash that wasn't correctly separated by harvester mechanism will conveying from sugarcane harvester to the truck and delivery to the sugar mill.

2.2 SUGAR PROCESSING

After being harvested in the southern region of Japan, sugarcane is typically transported to a sugar mill via truck. The sugar mill then undergoes three primary

processes: payment, raw sugar production, and refined sugar production. During the payment process, farmers are compensated for their crop before it is processed. Next, the sugarcane undergoes a raw sugar production process, where it is crushed and boiled to extract the raw sugar. Finally, the raw sugar is further processed and refined to produce the final sugar product.

2.2.1 The payment processes

The payment process for sugarcane involves objective methods of valuation, which typically include weighing and conventional techniques. Before the sugarcane is processed by milling, the truck carrying it is driven to the sugarcane dump yard (as shown in Figure 2.4 and 2.5). At this point, the truck is stopped, and the farmer's registration number is identified. The sugarcane is then weighed, and a sample is randomly extracted from the truck using a core sampling crane. Typically, around 5-15 kg of the sample is collected and sent to a laboratory for testing to determine the sugar quality and trash ratio, which are used to establish the price (as shown in Figure 2.6). This process ensures that farmers receive a fair and objective price for their sugarcane, based on its quality and quantity.

Figure 2.4: The sugarcane dump yard

Figure 2.5: Picture of sugarcane at sugar cane dump yard

In the payment processing room, the sugarcane sample is first weighed, which includes both sugarcane and non-sugarcane components. The sample is then sent to a

table where a group of 4-10 workers clean and separate the sugarcane from any trash. The workers use a sickle (known as a "カマ; Kama") to remove green leaves, dry leaves, soft tops, and to cut suspicious sugarcane in half to check for any fermentation or disease. They divide the sugarcane billets from the non-sugarcane parts such as dirt, rocks, and other plants. After the cleaning process, the sugarcane is weighed again, and then shredded using a cutter grinder. The shredded cane sample is then analyzed for sugar quality using a benchtop Vis-NIR spectrometer. The truck's registered account is updated with data on the sugarcane yield, trash ratio, and sugarcane quality to determine the price. Once the payment processing is complete, the truck dumps the sugarcane in the courtyard and waits for milling. The entire process takes around 10-15 minutes per truck, but this time frame may vary based on several conditions and factors.

Figure 2.6: Payment processes in Japan sugar mill

During the process of separating the sugarcane from the trash, many different types of sugarcane trash (as shown in Figure 2.7) are found, including green sugarcane leaves, dry sugarcane leaves, sugarcane roots, sugarcane soft-tops, dirt, stones, and sugarcane infected with disease or fermentation. These sugarcane trash items can cause problems with sugar quality during the manufacturing process. Some

of the sugarcane trash can still produce sugar, but in low amounts, while others cannot produce any sugar at all.

Figure 2.7: Sugarcane trash that was removed by labour

After the completion of the payment processes, the truck moves to the sugarcane courtyard to dump the sugarcane. Depending on the amount of sugarcane delivered in a day, it may have to wait for a day or even a week before processing into raw sugar. This waiting period can affect the quality of the sugarcane.

In addition, labor costs have affected the profitability of sugarcane production. Consequently, this reduced efficiency affects sugarcane quality, yield, and value. Including trash such as green sugarcane leaves, dry sugarcane leaves, parts of the root parts, and soil[23] in the sugar mills causes problems in the payment processes as sugar content and trash percentage are critical indices in determining prices for the farmer. Trash separation from the sugarcane sample is a labor-intensive task. Human errors[24] may arise due to the subjectivity of the process and as a consequence of the 100–300 deliveries to the sugar mills daily. Each sugar mill in

Japan requires 4–10 workers to separate the trash. The industry needs to explore new tools and methods that function faster and more accurately than manual methods to assess the quality of the sugarcane delivered.

2.2.2 Raw sugar process

The production of raw sugar involves several complex and interdependent processes that require careful attention to detail and a deep understanding of chemistry and engineering principles. The five major steps in the process are juice extraction, juice purification, evaporation, crystallization, and centrifugation.

The first step is juice extraction, where sugarcane is passed through a set of crushing rollers to obtain the sugarcane juice. This juice contains various impurities such as fibers, minerals, and non-sugar organic compounds that need to be removed to produce high-quality raw sugar.

The next step is juice purification, which aims to remove the impurities from the juice. This is done through mechanical methods such as filtration and chemical methods such as heating and adding lime. The goal is to obtain a clear, pure juice that is suitable for the next steps in the process.

The third step is evaporation, where the purified sugarcane juice is heated and concentrated to remove most of the water. This is typically done using a series of evaporators, which progressively remove water until the juice becomes a concentrated syrup.

In the fourth step, crystallization, the syrup is sent to a vacuum pan, where it is boiled to remove more water until it reaches the point of saturation. At this point, sugar crystals begin to form and are mixed with molasses, a thick, dark syrup that contains residual sugars and impurities.

The final step is centrifugation, where the massecuite mixture of sugar crystals and molasses is separated using a centrifuge machine. The sugar crystals are separated from the molasses and dried, resulting in the production of raw sugar.

Throughout the entire process, there are numerous challenges that must be overcome to ensure high-quality raw sugar production. These challenges include maintaining the correct temperature and pressure in the evaporators, ensuring that the juice is properly purified, and controlling the crystallization process to achieve the desired crystal size and purity.

In addition, the quality of the sugarcane itself can have a significant impact on the final product. Factors such as soil quality, climate, and pest control can all affect the sugar content and purity of the sugarcane, which in turn affects the quality of the raw sugar produced.

Overall, the production of raw sugar is a complex and challenging process that requires a combination of scientific knowledge, engineering expertise, and careful attention to detail. Despite these challenges, raw sugar production remains a critical industry, providing an essential ingredient for many food and beverage products around the world.

2.2.3 Refine sugar process

After the raw sugar is obtained from the manufacturing process, it is sent to the refined sugar factory to be processed into white sugar. The production of white sugar is a complex process that involves several steps, each designed to remove impurities and improve the quality of the sugar.

The first step in the production of white sugar is melting. This involves mixing the raw sugar with hot water or green molasses from spinning using sugar centrifugal

machine. The mixture obtained is called magma, which will later be centrifuged to remove the green molasses or molasses. The Affiliated Syrup obtained from the centrifuge will then be dissolved again to dissolve any remaining crystals that might have been undissolved from the churning process.

The next step is clarification, which is necessary to remove any impurities that may be present in the Affiliated Syrup. The syrup is passed through a sieve to mix with lime access bleaching in a bleaching pot. Then, it will filtrate by a pressure filter to separate the sediment and be bleached again for the last time by the Ion Exchange Resin process to obtain Fine Liquor. This ensures that the syrup is completely clear and free from any unwanted particles.

After the syrup has been clarified, it undergoes crystallization. The syrup will be fed into a vacuum pan to evaporate the water until the syrup reaches a saturation point and centrifuged to get refined sugar crystals and white sugar. The resulting sugar crystals are then separated from any remaining molasses using a centrifugal machine. The centrifuged sugar crystals are then rinsed and washed to remove any remaining impurities.

The final step in the production of white sugar is drying. The refined sugar crystals are baked by a dryer to remove any remaining moisture and ensure that the sugar is completely dry. The dried sugar crystals are then packed into sacks for sale. This process is essential in maintaining the quality of the sugar and ensuring that it is suitable for consumption.

In conclusion, the production of white sugar involves several complex steps that are necessary to remove impurities and improve the quality of the sugar. The refining process ensures that the sugar is pure, free from impurities, and suitable for consumption. It is important to note that the quality of the sugar produced is

dependent on the quality of the raw sugar, and any defects or impurities in the raw sugar can affect the final quality of the white sugar. Therefore, it is essential to ensure that the raw sugar is of high quality and free from any defects.

2.3 SPECTROSCOPY

Spectroscopy is a powerful analytical tool that is widely used in many fields, including chemistry, physics, biology, and material science. It provides valuable information about the structure, composition, and properties of materials based on the way they interact with light. Spectroscopy techniques have evolved over the years, and today, there are many different methods available, including infrared spectroscopy, ultraviolet-visible spectroscopy, Raman spectroscopy, and X-ray spectroscopy, among others. Each of these methods has its own strengths and limitations, and they can be used to study a wide range of materials, from small molecules to complex biological systems.

In spectroscopy, the spectrum is a critical piece of information that provides insight into the material being studied. The spectrum is a graph that shows how much light is absorbed, reflected, or transmitted by the material at different wavelengths. The intensity of the light is plotted on the y-axis, while the wavelength is plotted on the x-axis. By analyzing the spectrum, scientists can identify the spectral signature of the material, which is unique to that substance[3].

Equation (1), The Beer-Lambert law is a fundamental equation that is used to describe the relationship between the amount of light absorbed by a material and the concentration of the analyte in the material. The equation states that the absorbance of a material is proportional to the concentration of the analyte and the path length of

the light passing through the material. This law is widely used in spectroscopy to determine the concentration of a substance in a sample.

In conclusion, spectroscopy techniques are essential in many scientific fields, and they provide valuable information about the properties and composition of materials. By analyzing the spectral signature of a material, scientists can gain insight into its structure and behavior, and the Beer-Lambert law provides a fundamental equation that is used to determine the concentration of analytes in materials. As technology advances, new spectroscopy techniques and methods will continue to emerge, further expanding our understanding of the world around us.

$$A = \varepsilon Cl = \log\left(\frac{I_0}{I}\right) = -\log\left(\frac{I}{I_0}\right) \quad (1)$$

Where A is absorbance, ε is absorptivity (L $mol^{-1}cm^{-1}$) that is used for measure of how well a compound absorbs a given wavelength of light, C is concentration (in mol L^{-1}), l is path length (cm) or distant length that light has to travel through the sample, I_0 is intensity of incident energy as it enter the sample, and I is the intensity of reflected light or intensity as it leave the sample.

2.3.1 Overtone band

Overtone bands play an important role in the analysis of vibrational spectra of molecules. These bands arise due to the transitions of molecules from their ground state to the second excited state. This transition results in an increase in vibrational

quantum number (v) by 2. In comparison to fundamental bands, overtone bands occur at higher energies and shorter wavelengths.

Overtone bands are used to identify the presence of molecules in a sample and provide information about their vibrational modes. The intensities of overtone bands are generally weaker than fundamental bands, making them more challenging to detect. However, advancements in instrumentation and signal processing techniques have made it possible to detect and analyze these weak signals.

Moreover, overtone bands can also provide insights into the physical and chemical properties of the sample. For instance, the positions and intensities of overtone bands can be affected by factors such as hydrogen bonding, solvent interactions, and molecular symmetry. Therefore, the analysis of overtone bands can be used to study molecular interactions and understand the behavior of molecules in various environments.

In summary, overtone bands are an essential component of vibrational spectra and provide valuable information about the molecules in a sample. The study of overtone bands can be used to identify molecules, understand their vibrational modes, and investigate their physical and chemical properties. As a result, overtone bands are widely used in various fields, including chemistry, physics, and material science.

2.3.2 Main spectrometer components in present

In industrial settings, the spectrometers used for various applications usually have electronic components.

Detectors

One of the critical components of a spectrometer is the detector, which is responsible for detecting the light signals transmitted from the sample. Detectors can be divided into two main types: photo-emissive and solid-state detectors[3]. Photo-emissive detectors are typically represented by photomultiplier tube detectors, which are known for their high sensitivity and fast response times. On the other hand, solid-state detectors include photodiode detectors, pyroelectric detectors, and infrared detectors. The choice of detector depends on the specific requirements of the study or application, such as the wavelength range of interest or the required sensitivity.

Light source

Another important component of spectrometers is the light source, which is responsible for producing the electromagnetic radiation that interacts with the sample. Several materials can emit electromagnetic radiation, such as quartz tungsten-halogen monofilament lamps, pulsed xenon arc lamps, carbon arcs, and mercury lamps. The selection of the light source is based on the specific requirements of the study or application, such as the wavelength range of interest or the required intensity of the light. For example, a halogen lamp may be used for the visible to near-infrared (Vis-NIR) range, while other sources may be more suitable for other wavelength ranges.

In addition to detectors and light sources, spectrometers also contain other components such as optical fibers, gratings, and lenses. Optical fibers are used to transmit light signals from the sample to the detector, while gratings and lenses are used to separate the different wavelengths of light and focus the light onto the sample, respectively. The selection of these components is also based on the specific

requirements of the study or application. For instance, the choice of grating depends on the wavelength range of interest and the required resolution of the spectrometer.

Overall, the choice of components for spectrometers depends on various factors such as the specific application, the required sensitivity, the wavelength range of interest, and the required resolution. Advancements in technology have led to the development of more sophisticated components and instruments, enabling more accurate and reliable measurements in a variety of industrial and scientific settings.

2.4 NEAR-INFRARED SPECTROSCOPY IN SUGARCANE

Spectroscopy widely used in food and agricultural industries because they are fast, accurate, and cost-efficient. Normally spectroscopic techniques used the instrument call "spectrometer" to splits the incoming light into a spectrum for analytics, developing a calibration model, detection, and identification. The peak of absorbance spectrum line mean light source cannot receive much through the detector due to most of the light absorbed by the sample. Sugarcane mostly has O–H bonds overtone within 700–970 nm[25] of absorption ranges, and C-H overtone within 1700-1800 nm[4, 26] of absorption ranges which correspond to the biological signatures of materials such as water and sugar content[3, 25] Nowadays, some spectrometers are smaller and can work outside the laboratory.

2.5 SPECTRA CORRECTION AND SPECTRA PRE-TREATMENT

Spectral pre-treatment techniques play a crucial role in spectroscopic analysis as they help in improving the accuracy and reliability of the data. The pre-treatment technique involves many analytical methods that aim to correct the variables measured for a given sample that are subject to overall scaling or gain effects. These

effects are caused by various factors, including pathlength effects, scattering effects, source or detector variations, or other general instrumental sensitivity effects. The relative value of variables is often used in multivariate modelling rather than the absolute measured value to account for these scaling differences. Additionally, spectral pre-treatment methods also help to reduce unwanted noise and interference from the signals obtained from the sample. Some commonly used spectral pre-treatment methods include baseline correction, smoothing, normalization, and derivative transformation. These methods aim to enhance the spectral signals and improve the signal-to-noise ratio, thereby improving the accuracy and precision of the analysis.

2.5.1 Spectra correction (Absorbance)

The raw spectra collected from the portable Vis-NIR spectrometer were transformed into absorbance spectra using Eq. (2).

$$A = S_a = -\log\left[\frac{S_r - S_d}{S_w - S_d}\right] \quad (2)$$

where S_a is the absorbance spectra, S_r is the raw spectra, S_d is the dark reference spectra, and S_w is the white reference spectra scanned on the Teflon white reference plate.

2.5.2 Noise, Offset, and Baseline Filtering

Noise, offset, and baseline filtering techniques were performed to remove noise (high frequency) or background (low frequency) by utilizing the relationship between variables (Variables that are related to each other and contain similar information) in a data set.

Differentiation

Derivatives are the most common spectral pre-treatments technique. That is mainly used to resolve peak overlap (or enhance resolution) and eliminate constant and linear baseline drift between samples. Spectral derivatives calculated by obtaining the differences between two consecutive points or by smoothing/differentiating, specified gap distance, or Savitzky-Golay polynomial fitting[27]. However, the derivatives are noise enhancement and difficult spectral interpretation.

2.5.3 Normalization

The normalization methods attempt to give all samples an equal impact on the model[28]. Without normalization, some samples may have such severe multiplicative scaling effects that they will not be significant contributors to the variance and will not be considered necessary by many multivariate techniques. The ability of a normalization method to correct for multiplicative effects depends on how well one can separate the scaling effects, which are due to properties of interest from the interfering systematic effects.

Standard Normal Variate

Standard Normal Variate (SNV) is a pre-treatment method that effective in minimizing baseline offsets, compensate for light scattering effects, changes in path length, and multiplicative effects from absorbance spectra. The outcome of SNV, in many cases, is very similar to Multiplicative Scatter Correction (MSC). The SNV can be applied on absorbance by using equation (3).

$$A_{ij}^{snv} = \frac{A_{ij} - \bar{z}_i}{SD} \qquad (3)$$

Where; i^{th} is the spectrum of the collection used for calculation, j^{th} is absorbance value counter of i^{th} spectrum, A_{ij}^{snv} is corrected absorbance value with SNV, A_{ij} is measured absorbance value, $\overline{z_i}$ is the mean absorbance value of the uncorrected i^{th} spectrum, SD is standard deviation of the absorbance values of i^{th} spectrum.

2.6 MULTISPECTRAL IMAGES AND VEGETATION INDEX

Multispectral imaging is a technique used to capture images of a scene in multiple spectral bands or wavelengths. It is widely used in remote sensing applications to study vegetation, including crop monitoring, land-use mapping, and forest monitoring. Vegetation reflects and absorbs light differently at different wavelengths, allowing for the development of vegetation indices to quantify vegetation health and density. Multispectral images and vegetation indices provide valuable information for precision agriculture, environmental monitoring, and land-use management.

2.6.1 Multispectral imaging

Multispectral imaging is a spectroscopic technique that combines spectroscopy with digital imaging technologies. By capturing the light reflected from objects using a multispectral camera, spectral and spatial information of the object can be obtained, resulting in an image with wavelengths ranging from the visible to near-infrared spectrum. Multispectral imaging has become widely accepted as a fast, visual, and non-destructive technique in food and agricultural research.

Image processing techniques are typically used for learning the presence of objects, detecting and measuring them, and identifying them. An image can be defined as a two-dimensional function, f(x,y), where x and y represent spatial (plane) coordinates, and the amplitude of f at any pair of coordinates (x,y) is referred to as the intensity or brightness. In more advanced cases, an image can be defined as a three or more-dimensional function that is used for measurement and analysis (Figure 2.8).

The quality of an image is directly proportional to the quality of the settings applied to it. To use a camera as a measuring device, it must be calibrated to the physical world. This is done by performing geometric calibration to correct lens distortion and color calibration using reference colors. In most cases, the acquired image from the camera is not directly processed within the application. Instead, it is pre-processed to reduce noise and enhance brightness and contrast, which improves the image quality for the specific task at hand.

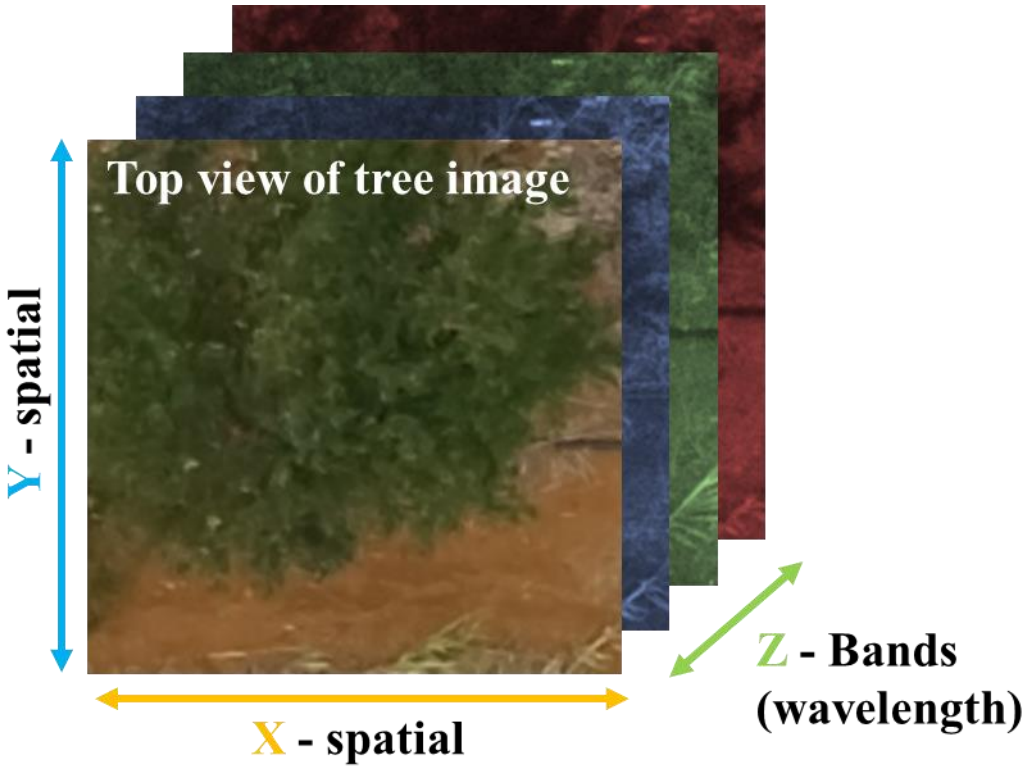

Figure 2.8: Example of RGB image

2.6.2 Vegetation index

Vegetation indices (VIs) are combinations of surface reflectance at two or more image bands that highlight specific vegetation properties[9]. NDVI, for example, is an index that distinguishes vegetation from other natural objects as it is moderately sensitive to leaf area index, high soil, and atmospheric background changes. $CI_{RedEdge}$ is used to calculate the chlorophyll content of plants, where RedEdge band are typically responsive to slight variations in chlorophyll content. NDVI, $CI_{RedEdge}$, and $SRPI_b$ are calculated using equations (4-6) as shown in Figure 2.9-2.11.

$$NDVI = \frac{(NIR-R)}{(NIR+R)} \quad (4)$$

$$CI_{RedEdge} = \left(\frac{NIR}{RedEdge}\right) - 1 \quad (5)$$

$$SRPI_b = \frac{B}{R} \quad (6)$$

Where R is the red band, G is the green band, B is the blue band, RedEdge is the RedEdge band, and NIR is the near-infrared band.

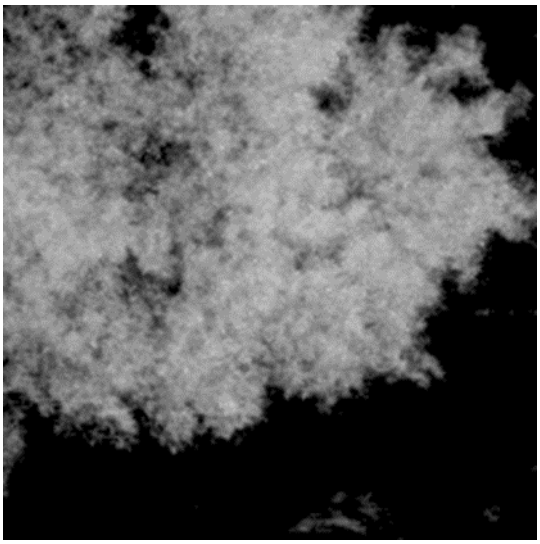

Figure 2.9: Example of NDVI image

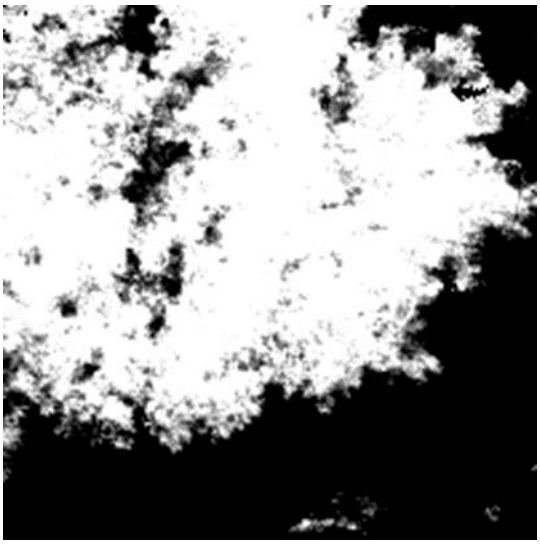

Figure 2.10: Example of $CI_{RedEdge}$ image

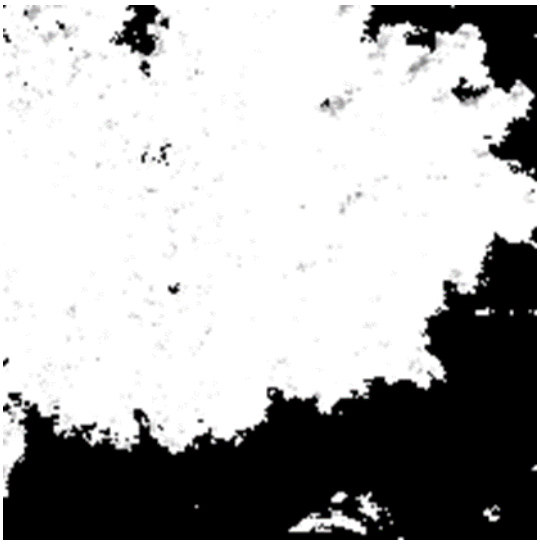

Figure 2.11: Example of $SRPI_b$ image

2.7 MULTIVARIATE DATA ANALYSIS (CHEMOMETRICS)

Multivariate data analysis is a crucial aspect of research in various fields, including chemistry, biology, economics, and more. This analytical approach involves analyzing and interpreting datasets with multiple variables simultaneously. Multivariate data analysis techniques provide an opportunity to extract more information from the data, including descriptive analysis, discrimination, and classification, and regression and prediction. Depending on the objectives of the study, various methods can be used. In this study, the aim was to develop regression models, and two methods were employed: Partial Least Squares Regression (PLS-R) and Multiple Linear Regression (MLR).

2.7.1 PLS-R and MLR

PLS-R generates a model by maximizing the covariance between the predicted and observable variables. This approach is particularly useful when the number of variables is large, and there is a potential for multicollinearity. On the other hand, MLR generates a model by fitting a linear equation to the data. It is particularly

sensitive to small changes in the data and can result in drastic changes in the regression coefficients. In summary, multivariate data analysis is a powerful tool that enables researchers to extract valuable insights from complex datasets. By selecting appropriate techniques, researchers can generate robust regression models that can help them make informed decisions.

The developed regression models were evaluated using the coefficient of determination (R^2), root mean square error of calibration (RMSEC), root mean square error of cross-validation (RMSECV), root mean square error of prediction (RMSEP), and bias.

$$Y=XT+E \tag{7}$$

where Y is the predicted Pol value, X is the sugarcane spectrum, T is the regression vector, and E is the residual.

$$y = \beta_0+\beta_1 x_1+\ldots+\beta_n x_n+\varepsilon \tag{8}$$

where y is the predicted Pol value, β_0 is the intercept regression coefficient, β is the regression coefficient, x is the selected wavelengths, ε is a model error, and n is the number of factors selected by a step-up method.

2.7.2 Validation

The prediction accuracy and precision could not know without checking it first when creating a model for calibration. The practical validation is the method to check how good the calibration by using a test set (external validation) when to have enough data or cross-validation (internal validation). Set of data can be select

manually or using algorithm up on user, Kennard-stone algorithm[29] to select the train and test set. In the case of cross-validation (CV), many techniques can be applied. For example, in the case of low number of data, leave-one-out-CV was the most useful for due to not complicate algorithm but have to careful when using with large data size due to it can result in overfit. Venetian blinds CV is an easy and relatively quick method appropriate for a large number of samples.

Coefficient of determination (R^2)

The coefficient of determination is a number between 0 and 1 that measures how well model predicts. The coefficient of determination (equation 9) can be calculated by square root of pearsons correlation coefficient (r) formular.

$$R^2 = \frac{n(\sum xy)-(\sum x)(\sum y)}{\sqrt{\left[n\sum x^2-(\sum x)^2\right]\left[n\sum y^2-(\sum y)^2\right]}} \quad (9)$$

Root Mean Square Error (RMSE)

RMSE, in equation 10, is defined as the average of the squared differences between predicted and measured Y-values of the validation one of the factors used to find the best model.

$$RMSE = \sqrt{\frac{\sum_{i=1}^{n}(y_i^{meas}-y_i)^2}{n}} \quad (10)$$

Bias

Bias is commonly used measure of the accuracy of a prediction model and use to check difference between calibration and validation set. The bias can be computed by using equation (11).

$$\text{Bias}=\frac{\sum_{i=1}^{n}(y_i^{meas}-y_i^{pred})}{n} \quad (11)$$

2.8 REVIEW RELATED WORK

The success of any research project is often built upon the foundation laid by previous studies in the same field. In this section, we aim to provide a comprehensive review of related works that have inspired the research at hand. By examining the previous studies, we can gain insights into the gaps and limitations of existing methods, identify areas where further research is needed, and ultimately build upon the knowledge and findings of previous researchers.

2.8.1 Networking system for sugarcane payment in Japan

The study conducted by Prof. Dr. Eizo Taira on the use of near-infrared spectroscopy for sugarcane in 2013 has led to significant advancements in the analysis of sugarcane samples. This study demonstrated the effectiveness of using NIR spectroscopy as a rapid and reliable method for quantitative analysis of shredded cane samples. As a result, an NIR network system for sugarcane was developed, which has since been adopted as the official method for determining cane prices in all raw sugar factories in Japan. The NIR network system provides accurate and efficient measurements of cane quality, allowing for quick and informed

decision-making by sugarcane producers and processors. The use of NIR spectroscopy in sugarcane analysis has revolutionized the sugar industry, offering a cost-effective and reliable alternative to conventional methods of analysis.

2.8.2 A portable Vis-NIR spectrometer for sugarcane research

In 2013, Prof. Dr. Eizo Taira conducted a collaborative study with HKN company to develop a portable Vis-NIR spectrometer specifically for sugarcane[6]. This study aimed to provide a portable and efficient method for the quantitative analysis of sugarcane quality, which can be measured both in the field and laboratory without causing any damage to the crop. The development of the portable Vis-NIR spectrometer has shown to be a significant advancement in the sugarcane industry as it has allowed for easy and rapid monitoring of sugarcane quality, thus improving harvest schedules and overall crop yield. The results of this study have been widely implemented in the sugarcane industry, resulting in better-quality sugar products and increased efficiency in the production process. Additionally, this technology has opened up opportunities for researchers to further explore the applications of Vis-NIR spectroscopy in other agricultural industries, leading to the development of more portable and accurate devices for field and laboratory analysis.

2.8.3 Unhealthy sugarcane detection using Vis-NIR spectra

In recent years, plant health monitoring has emerged as a promising application of spectroscopy. In 2022, the author conducted a study that revealed the potential of using spectroscopy for monitoring the health of sugarcane plants. The results of the study indicated that an unhealthy sugarcane can be detected using a portable Vis-NIR spectrometer with great accuracy and speed[30]. This discovery opens up new

possibilities for the development of a fully integrated monitoring system that could revolutionize the sugar industry. By leveraging the power of spectroscopy, such a system could offer real-time control over the monitoring of sugar industry operations, allowing for faster and more informed decision-making. The author's findings have laid the foundation for this idea, and further research in this direction could lead to significant advancements in the field of agricultural monitoring and management.

2.8.4 Hyperspectral imaging in sugarcane research

During their master's degree program in 2018, the author conducted a study on the use of hyperspectral cameras to identify and classify sugarcane trash, such as green leaves, dry leaves, rock, soil, and other materials. The findings of this research demonstrated the differences between the spectra of sugarcane and trash, highlighting the potential for using spectroscopy to separate or classify these materials based on their spectra[31]. This study served as inspiration for the author to pursue further research using spectroscopic imaging techniques, which led to the discovery of possible ways to spatially map sugar parameters on hyperspectral images of sugarcane[32].

2.8.5 Sugar quality prediction in sugarcane fields using UAS

Chea Chanreaksa conducted a study on sugar yield parameters and fiber prediction in small experimental sugarcane fields using a multispectral camera mounted on a small UAS. The research findings showed that three out of six vegetation indices (NDVI, $CI_{RedEdge}$, and $SRPI_b$) had a strong correlation with sugar

yield parameters[11], which served as inspiration for the author to conduct a similar experiment in a real sugarcane field.

Chapter 3: Research Design

This chapter outlines the research design adopted to achieve the aims and objectives stated in Section 1.3 of Chapter 1. The design includes several components, as follows:

Section 3.1: Experimental schematic

Section 3.2: Materials to be used in this study for data acquisition and analysis

Section 3.3: Acquisition of NIR spectra using a benchtop Vis-NIR spectrometer

Section 3.4: Acquisition of NIR spectra using a portable Vis-NIR spectrometer

Section 3.5: Reference analysis of sugar quality

Section 3.6: Preparation of datasets for the development of regression models for predicting sugar quality (first experiment)

Section 3.7: Preparation of datasets for the development of regression models for predicting sugar quality (second experiment)

Section 3.8: Field measurement and flight mission

Section 3.9: Background removal and region selection

Section 3.10: Preparation of datasets for the development of regression models for predicting sugar quality (third experiment).

This research design will provide a comprehensive framework for conducting experiments and analyzing data to achieve the research objectives.

3.1 EXPERIMENT SCHEMATIC

The objective of this study was to develop an evaluation system for sugarcane quality in Japan using a combination of instruments, including a polarimeter, refractometer, benchtop Vis-NIR spectrometer, portable NIR spectrometer, and a multispectral camera mounted on an unmanned aerial vehicle. To achieve this objective, the experimental methods were divided into three parts (see Figure 3.1):

In the first part of the study, a sugarcane quality calibration model was developed for the benchtop Vis-NIR spectrometer using spectral analysis results of sugarcane juice and sugarcane quality as measured by conventional methods.

The second part involved developing a sugar quality calibration model for a portable Vis-NIR spectrometer using stalk spectra and the sugar quality predicted from sugarcane juice using the benchtop Vis-NIR spectrometer.

In the final part of the study, a sugarcane quality map was developed for a multispectral camera mounted on a UAS using various cropped sizes of sugarcane canopy reflectance at the region of interest images and sugarcane quality as measured by a portable Vis-NIR spectrometer.

By developing these calibration models, the study aimed to provide an efficient and cost-effective way of evaluating sugarcane quality in Japan.

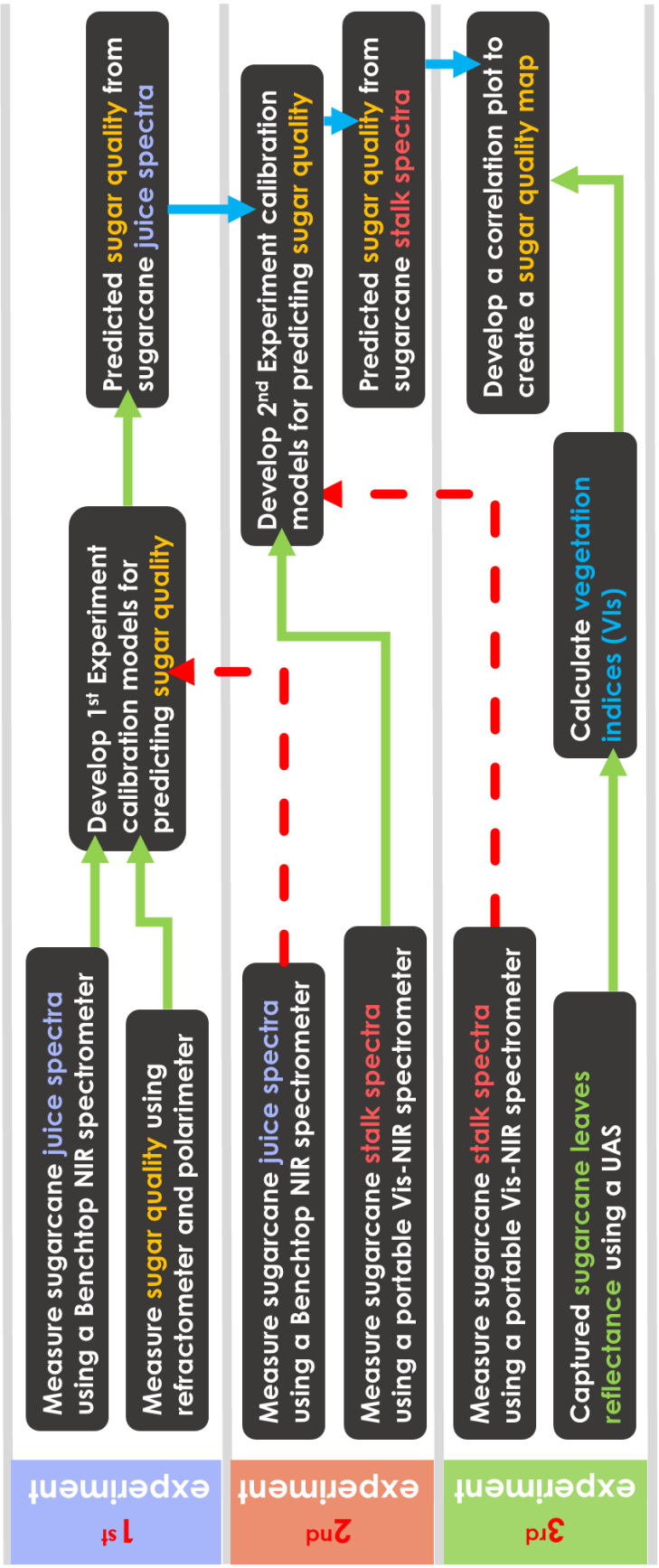

Figure 3.1: Experimental Schematic

3.2 MATERIALS

In the first experiment, Sugarcane billet samples from 16 sugar mills from the south of Japan were sent to the University of the Ryukyus, Okinawa for calibration during the 2020/2021 harvest season. The sugarcane billet samples were prepared, cut into 30-cm pieces, and pressed using a hydraulic press (Matsuo, Kagoshima, Japan) at 25.5 MPa for 1 min to extract a total of 213 sugarcane juice samples. Their absorption spectra and sugar quality were measured using both the benchtop Vis-NIR spectrometer and conventional method (Figure 3.2). In the second experiment, 103 sugarcane stalks were scanned at the sugarcane field using a portable Vis-NIR spectrometer and then harvested, cut into halves (approximately 30 cm each), and moved to the laboratory to press using the same settings as in the first experiment to extract sugarcane juice for obtaining sugarcane spectral information using the benchtop Vis-NIR spectrometer (Figure 3.2). This experiment was first conducted in the sugarcane experimental field at the University of the Ryukyus, Okinawa, Japan (Oct–Dec 2020).

In the last experiment, 103 sugarcane stalks were scanned at the sugarcane field using a portable Vis-NIR spectrometer and then harvested, cut into halves (approximately 30 cm each), and moved to the laboratory to press using the same settings as in the first experiment to extract sugarcane juice for obtaining sugarcane spectral information using the benchtop Vis-NIR spectrometer (Figure 3.2). This experiment was first conducted in the sugarcane experimental field at the University of the Ryukyus, Okinawa, Japan (Oct–Dec 2020).

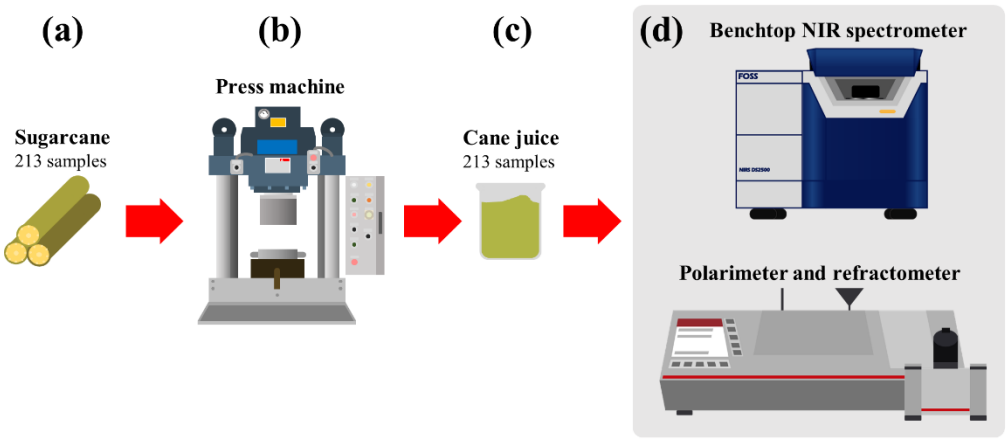

Figure 3.2: First experiment design outline: (a) Sugarcane billet samples were prepared by (b) pressing the stalks using a hydraulic press to extract (c) sugarcane juice to (d) measure Brix, Pol, and sugarcane spectra using a refractometer, polarimeter, and a benchtop Vis-NIR spectrometer.

3.3 ACQUISITION OF NIR SPECTRA OF THE BENCHTOP VIS-NIR SPECTROMETER

A 4.1-cm diameter measuring cup (slurry cup made of quartz) was filled with approximately 2 mL of each sugarcane juice sample and covered with a gold reflector (0.5 mm in size). Spectroscopic measurements were carried out twice for all samples using a benchtop Vis-NIR transmission spectrometer (DS2500; FOSS, Hillerød, Denmark). Distilled water was used for the zero (i.e., reference) setting. The Vis-NIR absorption was measured within the 400–2500-nm range in 0.5-nm increments. In the second experiment, the sugarcane juice measured twice was averaged into one spectrum.

3.4 ACQUISITION OF NIR SPECTRA OF A PORTABLE VIS-NIR SPECTROMETER

A portable Vis-NIR spectrometer (H-NIR-SC-01, HKN Engineering Co., Ltd., Wakayama, Japan) was used to scan the internode surface of the sugarcane stalk, once on the bottom and once on the top of the sugarcane stalk (Figure 3.3). This spectrometer was operated using a 25-W halogen lamp directly on a sugarcane stalk. A silicon array detector (spectral resolution of 462 channels) was used to detect the reflected light (Figure 3.4(b,c)). The spectral data are automatically transferred via Bluetooth to a Panasonic Toughbook (FZ-T1; Panasonic Corporation, Japan), where they are stored and displayed using a portable Vis-NIR spectrometer application. Figure 3.4(a) shows a portable Vis-NIR spectrometer of size 15.5×10.5×17 cm^3 (height×width×depth) and weight 1.19 kg. It contains a hand holder as well. The spectrometer is powered by four rechargeable lithium-ion batteries (NCR18650PF, Panasonic Corporation, Japan) and can measure spectra up to 5000 times. After the sugarcane was measured, it was harvested, pressed to extract the sugarcane juice samples to be quantified by the benchtop Vis-NIR spectrometer, and used as a validation set to test the calibration model of the first experiment (Figure 3.3). Next, the sugar quality was predicted using the calibration model and paired with the spectra determined using the portable Vis-NIR spectrometer, which was then used to develop calibration and validation models. NIR absorption was measured from 570 to 1031 nm in 1-nm increments. The spectra were measured with an integration time of 200 ms.

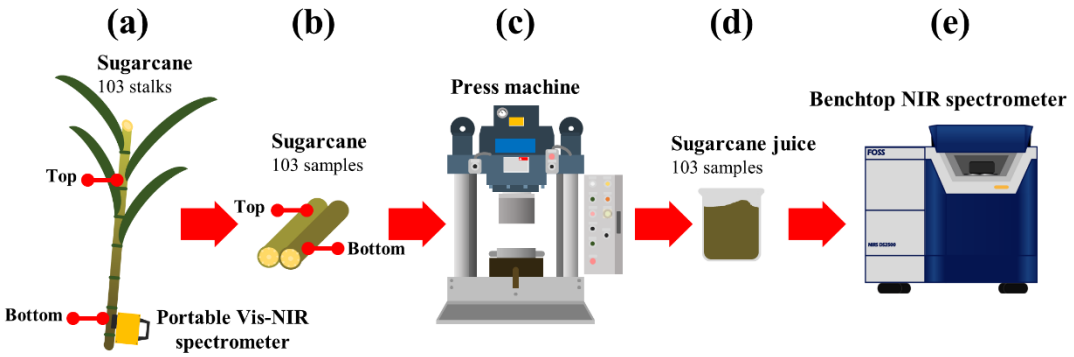

Figure 3.3: Second experiment design outline: (a) Scanning sugarcane stalk using a portable Vis-NIR spectrometer for sugarcane spectra. Then, (b) the sugarcane was harvested and prepared for (c) use in a hydraulic press to extract (c) sugarcane juice to (d) measure sugarcane spectra using a benchtop Vis-NIR spectrometer.

3.5 REFERENCE ANALYSIS OF SUGAR QUALITY

After the sugarcane samples were pressed and the NIR spectral data were collected, approximately 2 mL of the sugarcane juice from each sample was used to measure the Brix value (%Brix) twice using a refractometer (Abbemat-WR; Anton Paar GmbH, Graz, Austria), using distilled water for the zero setting. Next, approximately 100 mL of the sugarcane juice was mixed with 1.5 g of lead acetate to separate the other organic and non-sugar components from the sugarcane juice (Horne's method). The sugarcane juice was then filtered using a 150-mm filter paper circles (filter paper qualitative No. 2; Advantec, Toyo Roshi Kaisha, Ltd., Tokyo, Japan)[2]. Pure sugarcane juice was analyzed twice using a polarimeter (MCP500; Anton Paar GmbH, Graz, Austria) to obtain Pol (%Pol). In the second experiment, the two measurements of the sugar quality were averaged into one value.

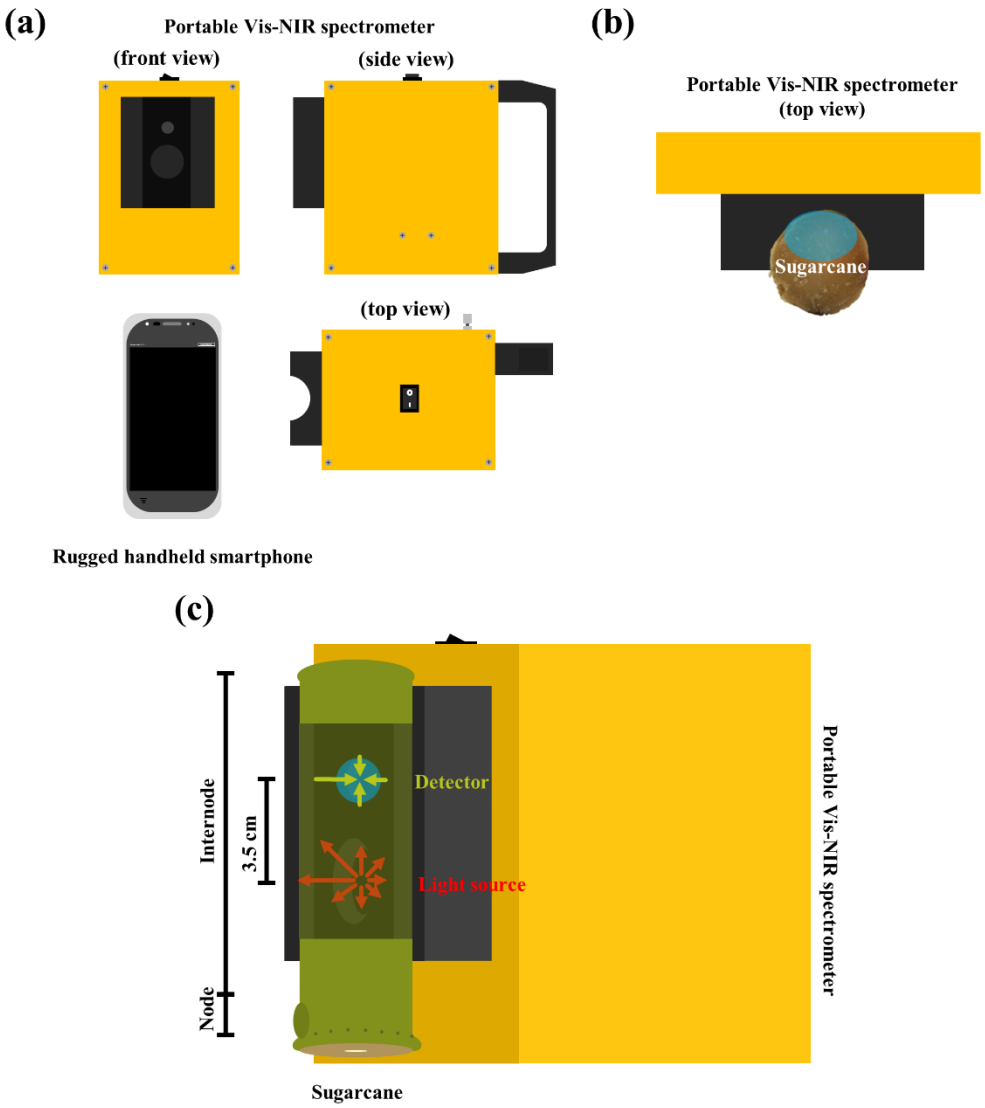

Figure 3.4: Portable NIR spectrometer. (b) Top view example of light transmission through sugarcane stalk. (c) An example of how a portable Vis-NIR spectrometer operates.

3.6 DATASET PREPARATION FOR THE DEVELOPMENT OF REGRESSION MODELS FOR PREDICTING SUGAR QUALITY (FIRST EXPERIMENT)

MATLAB R2021b (version: 9.11.0.1837725, The Math Works, Inc., USA) with PLS_Toolbox (version: 9.0, Eigenvector Research, Inc., USA) was utilized for data processing and analysis.

In the first experiment, 213 sugarcane juice spectra measured by the benchtop Vis-NIR spectrometer, and 213 sugar quality measurements obtained using the conventional method were used to develop six partial least square regression (PLS-R) models (no treatment, SNV, first derivative (D^1), second derivatives (D^2), D^1SNV, and D^2SNV). This dataset was then split into two groups: the first group contained 107 paired spectral and sugar quality values used as the calibration set, and the second group contained 106 paired spectral and sugar quality values used as the validation set according to the Kennard–Stone algorithm.

The number of data splits for venetian blinds cross-validation was set to two and the sample per blind was set to one, i.e., the samples were split into two test sets based on even and odd number of samples. Each test set was determined by selecting every data split in the dataset, starting at the first number of data splits.

The first experiment was developed only for the PLS-R model because the spectra of the benchtop Vis-NIR spectrometer exhibit high variability that can affect the regression coefficient of the MLR. The MLR technique used step-up search to select the wavelength in the ascending order based on the highest coefficient of regression between the actual sugar quality and the predicted one. However, this method removes a large amount of variable data from the spectra of the benchtop

Vis-NIR spectrometer, which might cause overfitting of the data. PLS-R model for prediction the sugar quality can be compute using equation (6).

3.7 DATASET PREPARATION FOR THE DEVELOPMENT OF REGRESSION MODELS FOR PREDICTING SUGAR QUALITY (SECOND EXPERIMENT)

The best regression model was then selected based on the highest coefficient of determination (R^2) with the lowest root mean square of prediction (RMSEP) and used for predicting the sugar quality of 103 sugarcane-juice spectral values determined in the second experiment. These 103 spectral values of the sugarcane stalk measured with the portable Vis-NIR spectrometer were paired with the predicted sugar quality to develop six PLS-R and multiple linear regression (MLR) models (no treatment, SNV, D^1, D^2, D^1SNV, and D^2SNV), where the samples of each model were divided into 52 calibration and 51 validation sets according to the Kennard–Stone algorithm. This experiment was developed using both PLS-R and MLR. It allowed the prediction of the sugar quality using equation (7) in the case of the PLS-R model and equation (8) in the case of the MLR.

3.8 FIELD MEASUREMENT AND FLIGHT MISSION

This study was conducted on three sugarcane fields on Minamidaitō Island, Okinawa, Japan, to gain data on sugarcane Pol and sugarcane canopy reflectance every month from September to December 2020. The sugarcane fields A, B, and C were 2.23, 2.40, and 1.00 ha, respectively. The sugarcane cultivar in fields A and B is Ni28 and RK97-14 in field C. At the start of the experiment, the sugarcane ages were approximately 8-11 months old.

Figure 3.5 shows six sugarcane stalks in the field were marked using ribbon as collection points to collect data of Pol and sugarcane canopy reflectance images at the same stalk. A portable Vis-NIR spectrometer was used to scan the internode surface of the sugarcane stalk (Figure 3.6) two times on the bottom and two times on the top to collect Pol of sugarcane and then average into one. A Panasonic Toughbook installed with a portable Vis-NIR spectrometer application was used to store and display data. Figure 3.7, The UAS (Phantom 4 multispectral, DJI, China) consists of one visible light camera and multispectral camera array with five cameras covering blue (450 ± 16 nm), green (560 ± 16 nm), red (650 ± 16 nm), red edge (730 ± 16 nm), and NIR (840 ± 26 nm). The multispectral image was TIFF-format, and the image size was 1600 x 1300 pixels with 16-bit depth. Figure 3.8, The DJI GS Pro application on an iPad was used to plan the flight mission, the height of the flight was set at 60 m above the ground, and the speed was set at seven m/s. A total of four flight missions were conducted during the experiment period: September 18th, October 15th, November 17th, and December 16th, 2020. All four flights were scheduled between 11:00 am and 3:00 pm. By the end of the experiment, a total of 72 (six points × four flights × three fields) data of sugarcane Pol and sugarcane canopy reflectance images were collected.

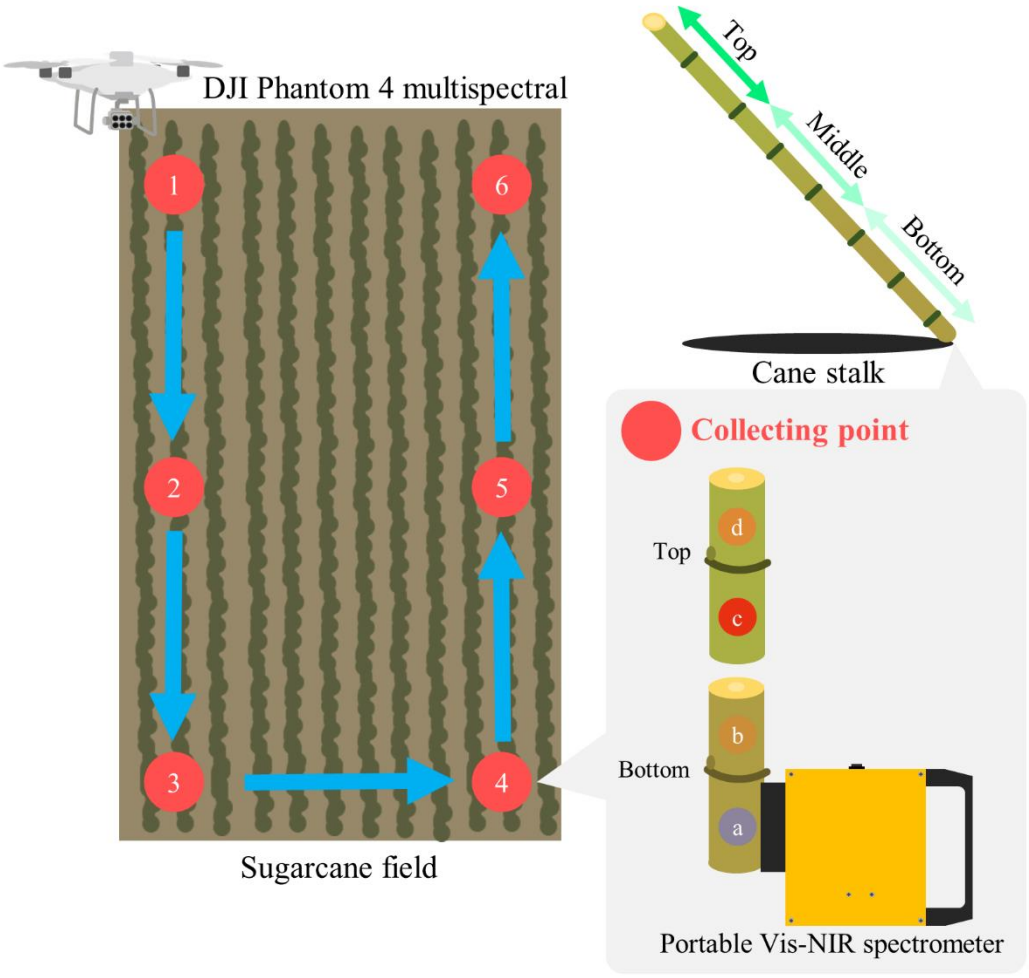

Figure 3.5: Example of the flight contour and details of using a portable Vis-NIR spectrometer to scan the sugarcane stalk twice on the bottom and top at the collection points.

Figure 3.6: Photo of using a portable Vis-NIR spectrometer to scan the sugarcane stalk.

Figure 3.7: Photo of deploying drone.

Figure 3.8: Photo of drone control using DJI GS Pro application.

3.9 BACKGROUND REMOVAL AND REGION SELECTION

Calculate the VIs (NDVI, $CI_{RedEdge}$, and $SRPI_b$) using sugarcane canopy reflectance image bands. After calculating the VIs, the soil background of all images was removed by the NDVI value and then cropped into four sizes of the image as shown in Figure 3.7: 50×50, 100×100, 150×150, and 200×200 pixels on the area of interest by manually selecting coordinate numbers at the collection points for ten times and averaging into one.

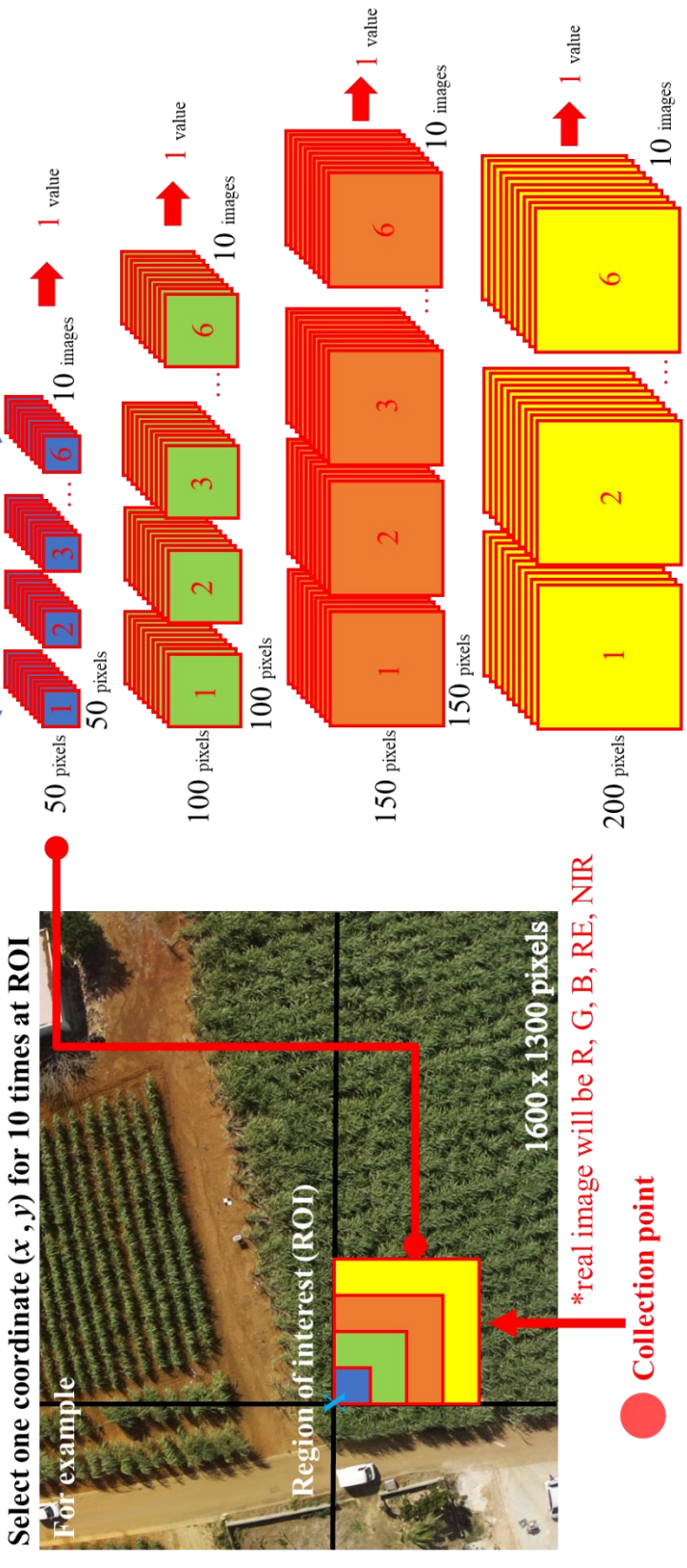

Figure 3.9: Example of cropped multispectral images.

3.10 DATASET PREPARATION FOR THE DEVELOPMENT OF REGRESSION MODELS FOR PREDICTING SUGAR QUALITY (THIRD EXPERIMENT)

This research has two main datasets. In the first set, 72 sugarcane Pol and VIs were averaged by six collecting points into 12 sugarcane Pol and VIs to develop the twelve simple linear regression (SLR) models. In the second set, 72 sugarcane Pol and image bands were averaged by six collecting points into 12 sugarcane Pol and image bands to develop the twenty MLR models.

Chapter 4: Results and Discussion

This chapter presents the results and discussion of the study, which followed the research design stated in Chapter 3. The sections below outline the findings of the study:

Section 4.1: discusses the absorbance spectra of sugarcane juice.

Section 4.2: describes the regression models developed using Brix and sugarcane juice spectra.

Section 4.3: presents the regression models developed using Pol and sugarcane juice spectra.

Section 4.4: presents the absorbance spectra of sugarcane stalk.

Section 4.5: describes the regression models developed using Brix and sugarcane stalk spectra.

Section 4.6: presents the regression models developed using Pol and sugarcane stalk spectra.

Section 4.7: examines the monthly trend of measured sugar quality using a portable Vis-NIR spectrometer.

Section 4.8: provides a summary of sugarcane canopy reflectance images.

Section 4.9: analyzes the monthly trend of vegetation indices.

Section 4.10: explores the correlation between sugar quality and three vegetation indices.

Finally, section 4.11: discusses the correlation between sugar quality and five image bands.

These sections provide a comprehensive analysis of the data and the findings, which will help in evaluating the sugarcane quality in Japan.

4.1 ABSORBANCE SPECTRA OF SUGARCANE JUICE

Figure 4.1 shows the average absorbance spectra of the sugarcane juice measured using the benchtop Vis-NIR spectrometer. The spectra have significant peaks at 480, 680, 970, 1190, 1450, 1790, 1930, and 2450 nm. The peak at 480 nm is a green band that at 680 nm is characteristic of the chlorophyll band, and those at 970, 1190, 1450, 1790, 1930, and 2450 nm show the water content of the sugarcane sample[33]. A previous study considered the main absorption peaks at 970, 1190, 1450, and 1790 nm for the analysis and developed a calibration model to measure sugar quality[4]. Therefore, our study used a band within 700–1850 nm. Figure 4.2 shows the average second derivative of the sugarcane juice absorbance spectra in the wavelength range of 700–1850 nm. The second derivative filter fixes the spectral baseline and enhances the peaks of sugarcane juice absorbance spectra, thereby aiding in a better visual comparison.

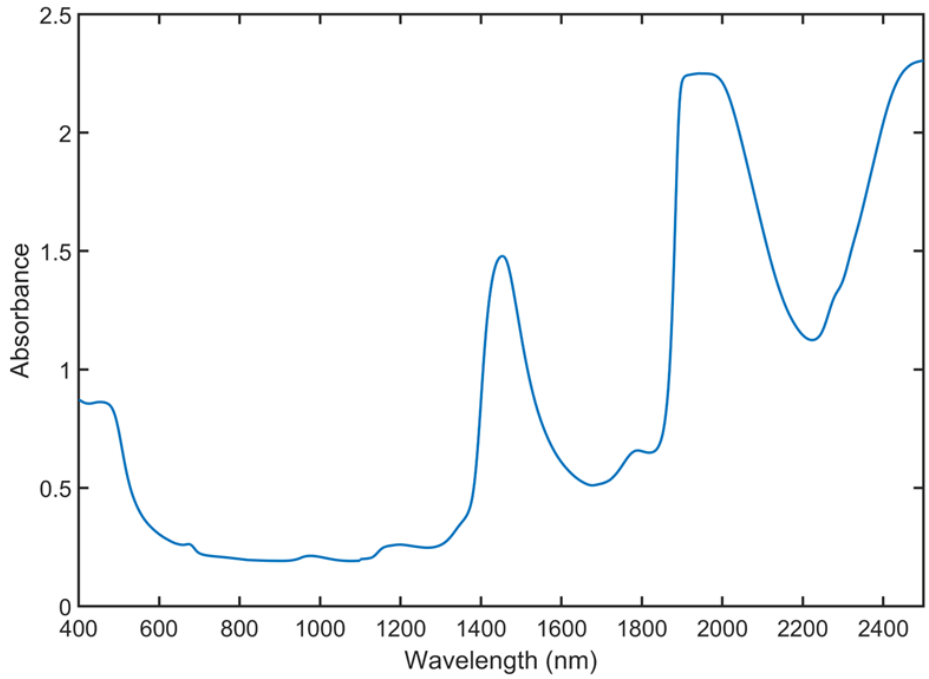

Figure 4.1: Average absorbance spectra of sugarcane juice in full wavelength range (400–2500 nm).

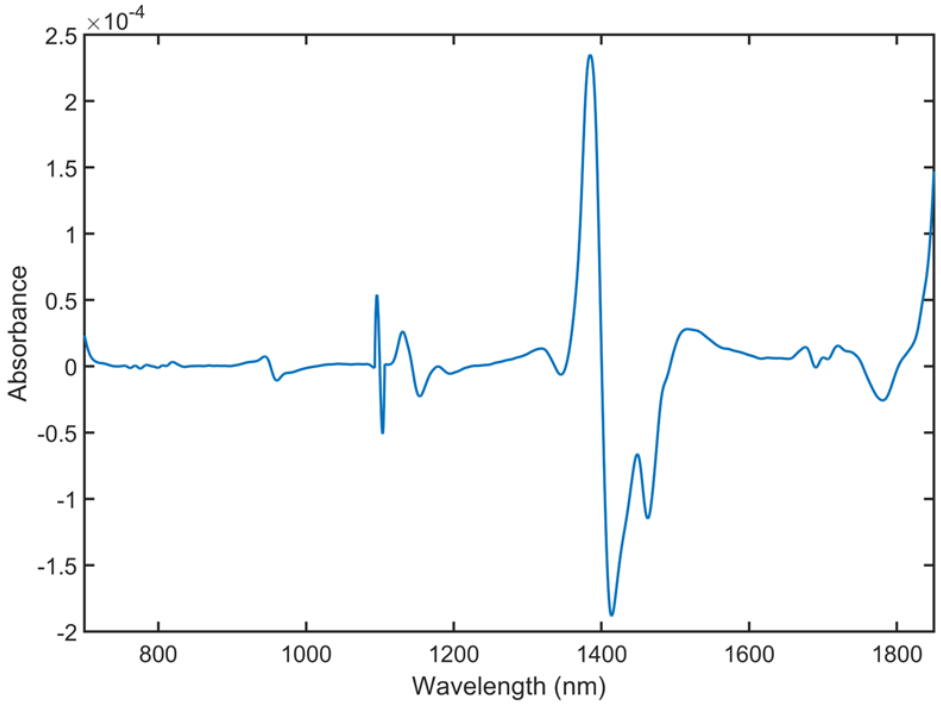

Figure 4.2: Second derivative of sugarcane juice absorbance spectra.

4.2 REGRESSION MODELS USING BRIX AND SUGARCANE JUICE SPECTRA

Characteristics of the Brix and Pol values of the sample set are listed in Table 4-1. Six regression models were developed: no treatment, SNV, D^1, D^2, D^1SNV, and D^2SNV. Table 4-2 shows the results of the regression model for Brix measurement. All models have high R^2_c ($\geq$0.98) because the NIR spectrum from the benchtop Vis-NIR spectrometer had low noise, and the spectrum line showed clear peaks. A comparison of the results of this calibration showed that the RMSEC of no-treatment and SNV-treatment models had slightly lower values than those of other models (no treatment = 0.2%, SNV = 0.2%, D^1 = 0.3%, D^2 = 0.3%, D^1SNV = 0.2%, D^2SNV = 0.3%). The RMSECV of no-treatment and SNV-treatment models were also lower than those of the other models (no treatment = 0.3%, SNV = 0.3%, D^1 = 0.3%, D^2 = 0.3%, D^1SNV = 0.3%, D^2SNV = 0.3%). Validation results indicated that the model developed with SNV had the lowest RMSEP (0.2%). Hence, SNV pre-treatment is effective for Brix calibration. Figure 4.3 shows the regression vector of the model with SNV pre-treatment. The key wavelengths employed to evaluate the Brix value using the sugarcane juice spectra were approximately 1102.5, 1125.5, 1433, 1579.5, and 1754.5 nm, which were close to the previous key wavelengths used to measure the sugar quality.

Table 4-1: Brix and Pol of juice used for calibration and validation. Samples were measured using a conventional method.

Component	Indicators	N	Average	Minimum	Maximum	Std.
Brix	Calibration set	107	20.3	15.0	24.9	2.1
(%Brix)	Validation set	106	20.3	15.3	24.8	2.1
Pol	Calibration set	107	17.9	12.0	22.6	2.2
(%Pol)	Validation set	106	17.9	12.0	22.5	2.2

N: number of samples; Std: standard deviation

Table 4-2: PLS-R results for predicting Brix using sugarcane juice spectra

Pre-treatment	LVs	Indicators						
		Calibration				Validation		
		R^2_c	RMSEC*	R^2_{cv}	RMSECV*	R^2_p	RMSEP*	bias*
None	8	0.99	0.2	0.99	0.3	0.99	0.3	-0.03
SNV	7	0.99	0.2	0.99	0.3	0.99	0.2	-0.05
D^1	6	0.99	0.3	0.98	0.3	0.98	0.3	-0.03
D^2	7	0.99	0.3	0.98	0.3	0.97	0.4	-0.03
D^1SNV	7	0.99	0.2	0.98	0.3	0.99	0.3	-0.03
D^2SNV	6	0.98	0.3	0.98	0.3	0.98	0.3	-0.02

LV: latent variable; R^2: coefficient of determination of calibration; RMSEC: root mean square error of calibration; RMSEP: the root mean square error of prediction; SNV: standard normal variate; D^1: first derivative; D^2: second derivative. *%Brix

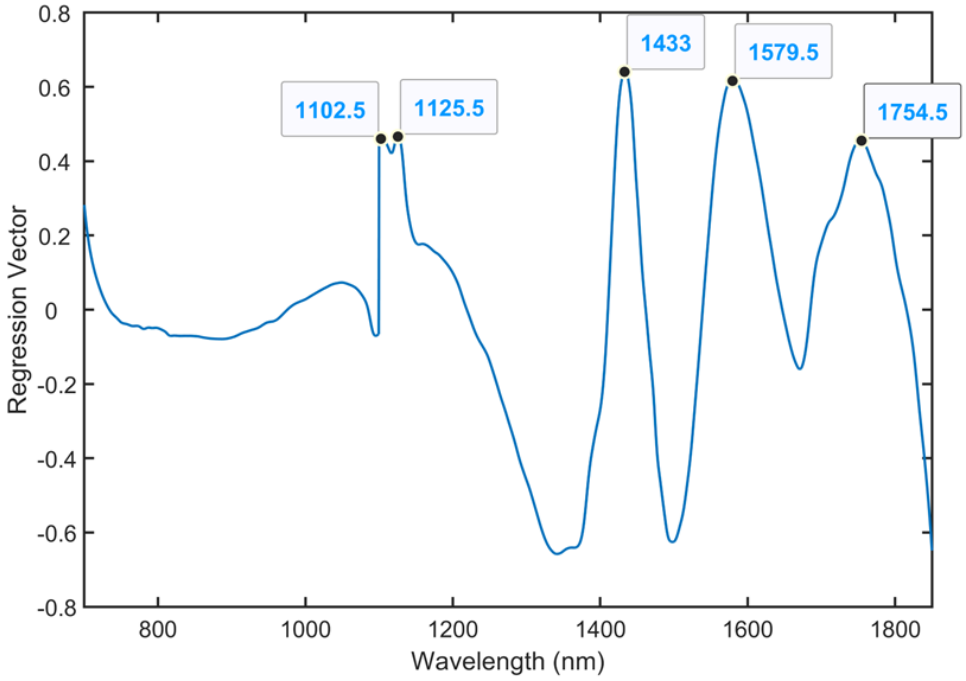

Figure 4.3: SNV pre-treatment regression vector of Brix.

4.3 REGRESSION MODELS USING POL AND SUGARCANE JUICE SPECTRA

The R^2_c of all models for Pol prediction are ≥0.96 (Table 4-3). A comparison of the calibration results showed that the RMSEC of the models with the second-derivative treatment (D^2 and D^2SNV) is slightly lower than that of the other models (no treatment = 0.5%, SNV = 0.4%, D^1 = 0.3%, D^2 = 0.2%, D^1SNV = 0.2%, D^2SNV = 0.2%). The RMSECVs of D^1SNV and D^2SNV treatments were also lower than those of the other models (no treatment = 0.6%, SNV = 0.5%, D^1 = 0.4%, D^2 = 0.5%, D^1SNV = 0.3%, D^2SNV = 0.4%). The validation results indicated that the model developed with the second-derivative pretreatment had the lowest RMSEP (0.3%). Hence, the second-derivative pretreatment is effective for Pol calibration. Figure 4.4 shows the regression vector of the model with the second-derivative pretreatment.

The key wavelengths to evaluate the Pol using the sugarcane juice spectra were 911, 1197.5, 1387, 1440.5, 1565.5, 1701, 1754.5, and 1779.5 nm, which are close to those required to measure the sugar quality.

Table 4-3: PLS-R results for Pol using sugarcane juice spectra

Pre-treatment	LVs	Indicators						
		Calibration set				Validation set		
		R^2_c	RMSEC (%Pol)	R^2_{cv}	RMSECV (%Pol)	R^2_p	RMSEP (%Pol)	bias (%Pol)
None	10	0.96	0.5	0.92	0.6	0.95	0.5	-0.00
SNV	10	0.97	0.4	0.96	0.5	0.97	0.4	0.02
D¹	10	0.99	0.3	0.97	0.4	0.98	0.3	0.04
D²	10	0.99	0.2	0.95	0.5	0.99	0.3	0.01
D¹SNV	10	0.99	0.2	0.98	0.3	0.98	0.3	0.02
D²SNV	10	0.99	0.2	0.97	0.4	0.98	0.3	0.00

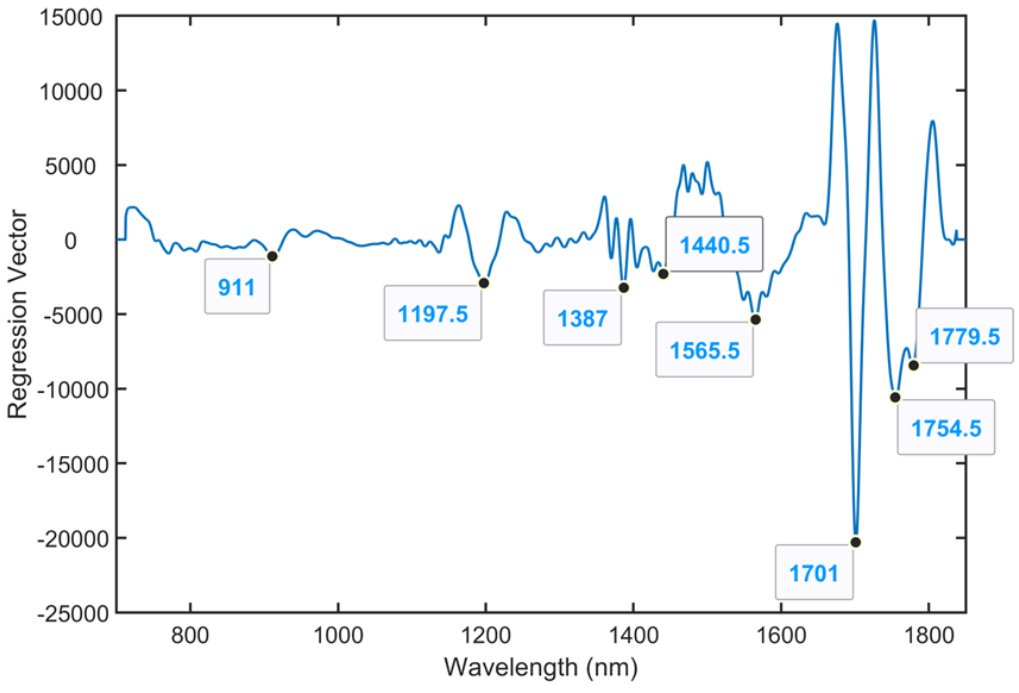

Figure 4.4: D^2 pre-treatment regression vector of Brix in the wavelength range of 700–1850 nm.

4.4 ABSORBANCE SPECTRA OF SUGARCANE STALK OBTAINED FROM THE PORTABLE VIS-NIR SPECTROMETER

As the starting and ending sections of the spectra obtained by the Vis-NIR spectrometer do not exhibit any peaks and show a similar trend, spectra in the wavelength range of 600–1000 nm were used. Figure 4.5 shows the average absorbance spectra of the sugarcane stalk measured each month with the portable NIR spectrometer. Figure 4.6 shows the average second derivative of the sugarcane stalk absorbance spectra in the wavelength range of 600–1000 nm. The second-derivative filter fixes the spectral baseline and enhances the peaks of the sugarcane juice. As a result, significant peaks at 650, 680, 740, 770, 846, 900, and 960 nm were obtained. The peaks at 650 and 680 nm are characteristic of the chlorophyll band, while those at 740, 770, 846, and 960 nm can be mainly attributed to the water[33], and that at 900 nm to the sugar content[34] of the sugarcane sample.

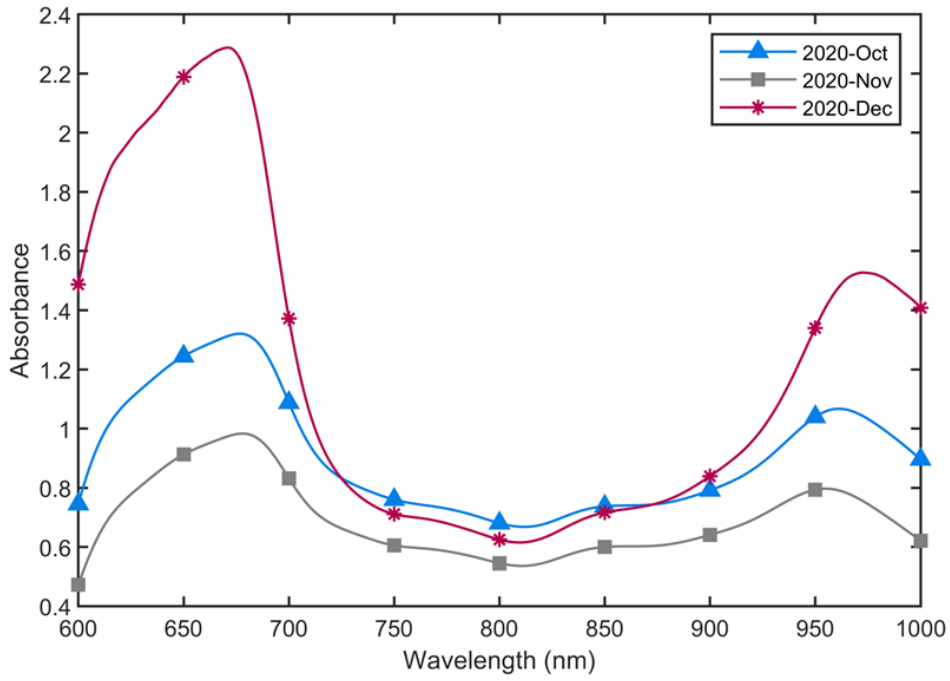

Figure 4.5: Average absorbance spectra of sugarcane stalk for each month.

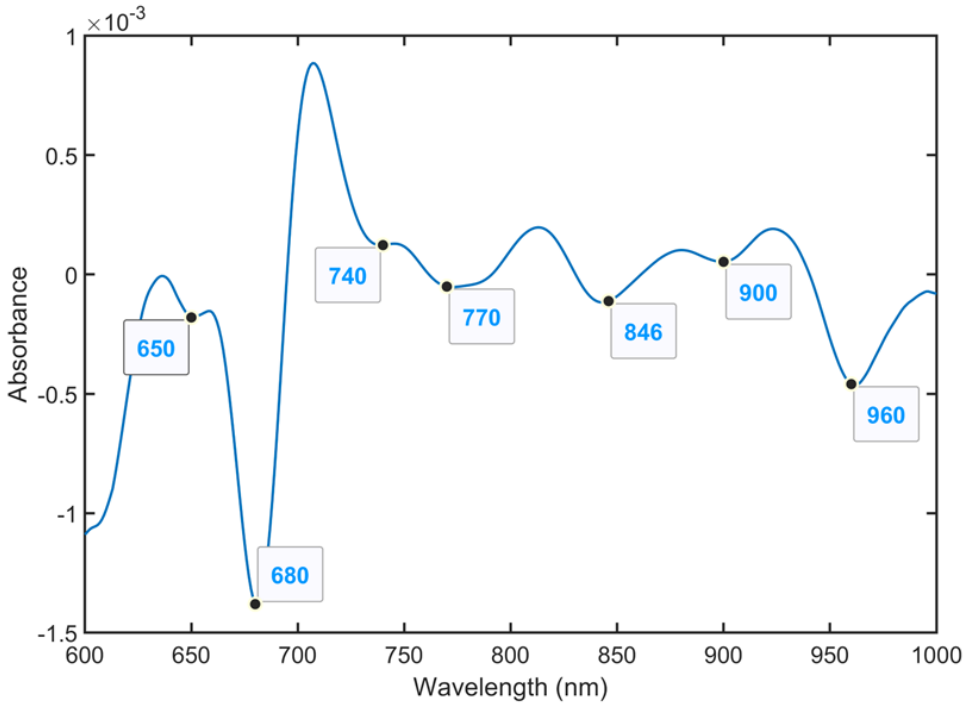

Figure 4.6: Average second derivative of sugarcane stalk absorbance spectra for three months.

4.5 REGRESSION MODELS USING THE PREDICTED BRIX AND SUGARCANE STALK SPECTRA

The predicted Brix and Pol values of the sample set obtained from the best calibration models of each value developed in the first experiment are listed in Table 4-4. Here, 24 regression models for Brix and Pol have developed: no treatment, SNV, D^1, D^2, D^1SNV, D^2SNV per PLS-R, and MLR. Table 4-5 shows the results of the regression models for Brix measurement using the Brix predicted from the best Brix model from the first experiment and the sugarcane stalk spectra measured by the portable Vis-NIR spectrometer. The R^2_c of all models is ≥0.70. A comparison of the calibration results showed that the RMSEC of the models with the MLR with the second-derivative treatment (D^2, D^2SNV) had the lowest value among the models

(D^2 = 1.0%, D^2SNV = 1.0%). Validation results indicated that the MLR model developed with the second-derivative pretreatment had the lowest RMSEP (1.4%). These results demonstrated that MLR with the second-derivative pretreatment is considerably effective for Brix calibration (R^2 = 0.70).

The MLR model with the second-derivative pretreatment indicates that five key wavelengths (944, 788, 653, 911, and 827 nm) can be used to predict the Brix using the sugarcane stalk absorbance spectra. Wavelengths of 944, 788, and 827 nm can be attributed to the water content, 653 nm to the chlorophyll content, and 911 nm to the sugar content of the sugarcane.

Table 4-4: Characteristic of Brix and Pol in juice values of calibration and validation development. Samples were measured from sugarcane juice spectra using benchtop Vis-NIR spectrometer

Component	Indicators	N	Average	Minimum	Maximum	Std.
Brix	Calibration set	52	20.3	14.0	25.3	2.6
(%Brix)	Validation set	51	20.3	15.6	24.8	2.5
Pol	Calibration set	52	17.9	11.0	22.6	2.6
(%Pol)	Validation set	51	17.9	12.8	22.6	2.5

Table 4-5: Result of PLS-R and MLR for predicting Brix in sugarcane stalk using sugarcane stalk spectra.

Model	Pre-treatment	LVs/Nf	Selected wavelengths (nm)					Indicators						
								Calibration set		Cross-validation		Validation set		
			1	2	3	4	5	R^2_c	RMSEC (%Brix)	R^2_{cv}	RMSECV (%Brix)	R^2_p	RMSEP (%Brix)	bias (%Brix)
PLS-R	None	4						0.72	1.4	0.70	1.4	0.57	1.7	-0.06
	SNV	5						0.75	1.3	0.69	1.5	0.60	1.6	-0.06
	D^1	3						0.70	1.4	0.68	1.5	0.62	1.5	-0.11
	D^2	4						0.75	1.3	0.67	1.5	0.63	1.5	-0.15
	D^1SNV	5						0.76	1.3	0.71	1.4	0.64	1.5	-0.11
	D^2SNV	4						0.72	1.4	0.67	1.5	0.57	1.7	-0.18
MLR	None	2	665	962				0.66	1.5			0.58	1.7	0.08
	SNV	2	938	697				0.57	1.7			0.55	1.7	-0.10
	D^1	5	667	982	768	793	621	0.78	1.2			0.59	1.6	-0.04
	D^2	5	944	788	653	911	827	0.84	1.0			0.70	1.4	0.03
	D^1SNV	5	834	817	683	778	663	0.71	1.4			0.58	1.6	0.01
	D^2SNV	4	956	869	756	679		0.85	1.0			0.70	1.4	0.14

PLS-R: partial least-squares regression; MLR: multiple linear regression; Nf: number of factors.

4.6 REGRESSION MODELS USING THE PREDICTED POL AND SUGARCANE STALK SPECTRA

The R^2_c of all PLS-R and MLR models of Pol developed using the Pol predicted from the best Pol model from the first experiment and the sugarcane stalk spectra measured by the portable Vis-NIR spectrometer were ≥0.63 and ≥0.64, respectively (Table 4-6). A comparison of the results for this calibration showed that the RMSEC of MLR models with the second derivative (D^2 and D^2SNV) had the lowest value (D^2 = 1.2, D^2SNV = 1.0%) and validation results. The PLS-R model with D^2SNV had the lowest RMSEP (1.4%). These results demonstrate that the MLR model with the second-derivative SNV pre-treatment is the most effective model for

Pol calibration. The MLR model with the second-derivative SNV pre-treatment shows that four key wavelengths (954, 869, 758, and 629 nm) can be used to evaluate the Pol in the sugarcane stalk absorbance spectra. Most of the selected wavelengths (954, 869, and 758 nm) can be attributed to the water and sugar contents of sugarcane.

Table 4-6: Result of PLS-R and MLR for predicting Pol in sugarcane stalk using sugarcane stalk spectra.

Model	Pretreatment	LVs/Nf	Selected wavelengths (nm)					Indicators						
								Calibration set		Cross-validation		Validation set		
			1	2	3	4	5	R^2_c	RMSEC (%Pol)	R^2_{cv}	RMSECV (%Pol)	R^2_p	RMSEP (%Pol)	bias (%Pol)
PLS-R	None	4						0.74	1.3	0.70	1.4	0.63	1.6	-0.01
	SNV	2						0.63	1.6	0.59	1.7	0.61	1.6	-0.09
	D^1	3						0.72	1.4	0.68	1.5	0.67	1.4	-0.04
	D^2	4						0.76	1.3	0.68	1.5	0.68	1.4	-0.07
	D^1SNV	5						0.77	1.3	0.70	1.4	0.67	1.5	-0.04
	D^2SNV	4						0.76	1.3	0.66	1.6	0.63	1.6	-0.09
MLR	None	2	600	978				0.73	1.4			0.62	1.6	0.10
	SNV	2	936	697				0.64	1.6			0.61	1.6	-0.06
	D^1	5	975	665	830	877	916	0.78	1.2			0.63	1.6	-0.13
	D^2	5	942	787	832	655	981	0.80	1.2			0.67	1.5	0.02
	D^1SNV	5	832	815	685	781	749	0.75	1.3			0.55	1.8	-0.03
	D^2SNV	4	954	869	758	629		0.84	1.0			0.70	1.4	0.05

4.7 THE MONTHLY TREND OF MEASURED SUGAR QUALITY USING A PORTABLE VIS-NIR SPECTROMETER

The changes in Pol value for sugarcane fields from September to December are displayed in Figure 4.7-4.9. As evident from the figures, the Pol value decreased across all fields from September to October due to the damage caused by tropical cyclones. In November, there was a noticeable improvement as the fields started to recover, leading to an increase in Pol value. However, it is important to note that the

error bars for Pol value across all fields during this period were highly variable, with six collecting points showing significantly different distributions. This variability can be attributed to the prolonged impact of the tropical storms in October and November, which persisted despite the recovery of the fields in November. By December, however, the effects of the storms had entirely disappeared, leading to a more consistent distribution of Pol value across all collecting points.

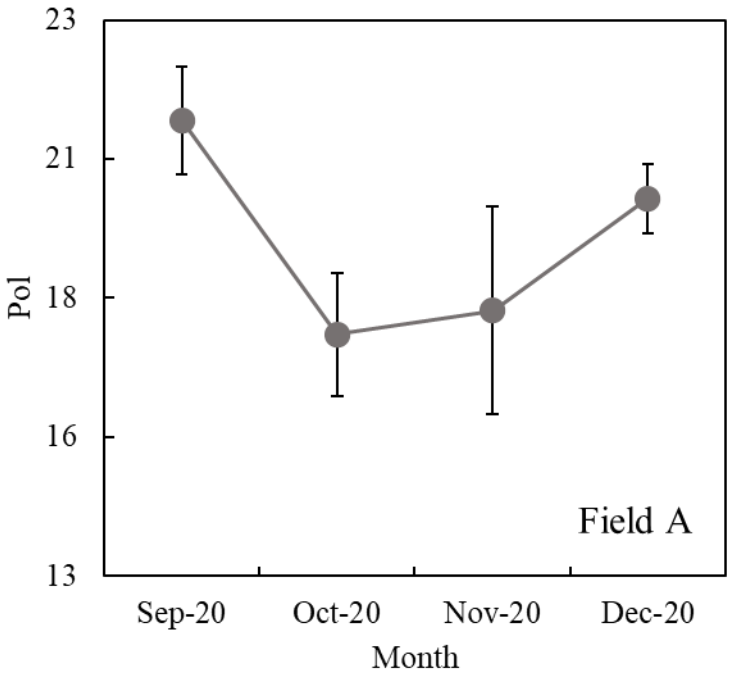

Figure 4.7: Average monthly trend of predicted Pol using a portable Vis-NIR spectrometer at Field A

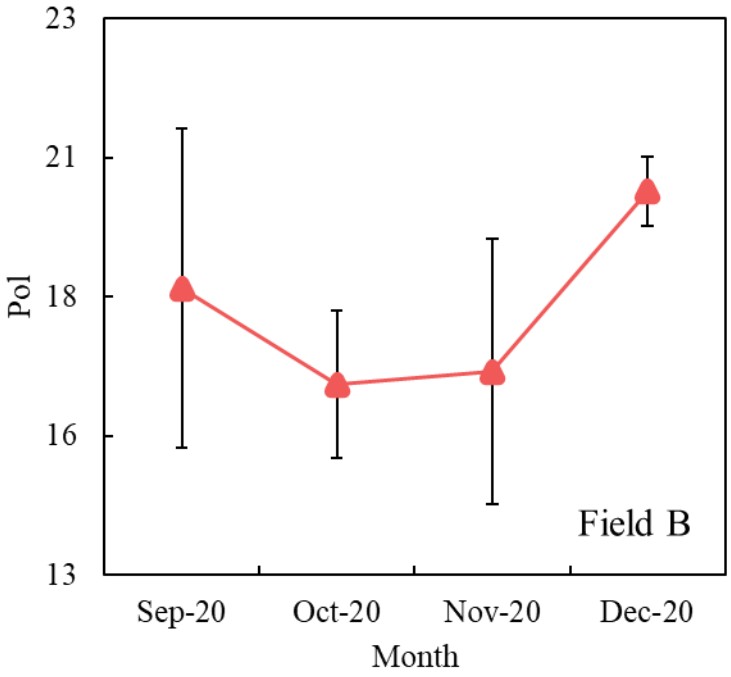

Figure 4.8: Average monthly trend of predicted Pol using a portable Vis-NIR spectrometer at Field B

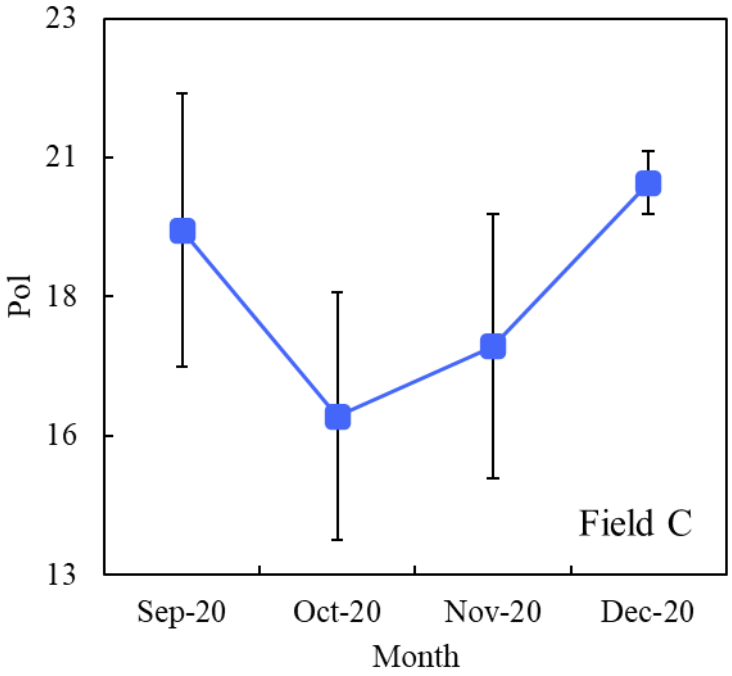

Figure 4.9: Average monthly trend of predicted Pol using a portable Vis-NIR spectrometer at Field C

4.8 SUMMARY OF SUGARCANE CANOPY REFLECTANCE IMAGES

The reflectance image bands for all sugarcane fields showed a consistent trend, although some slight differences were observed depending on image size. Figures 4.10-4.12 demonstrate that in September, the NIR image band value was lowest in Fields A and C, likely due to the greater damage caused by tropical cyclones in these fields, resulting in reduced cane density and changes to the sugarcane leaves. However, from October to December, the NIR image band value showed a similar pattern across all fields, indicating that the impact of the cyclones on Pol value varied depending on the location and level of damage within each field. Furthermore, our analysis revealed that most error bars for the 50×50 and 200×200 image sizes showed inconsistent results after ten rounds of manual selection, leading to instability in developing a calibration model. This finding highlights the need for more reliable image selection methods to ensure accurate calibration and reliable results.

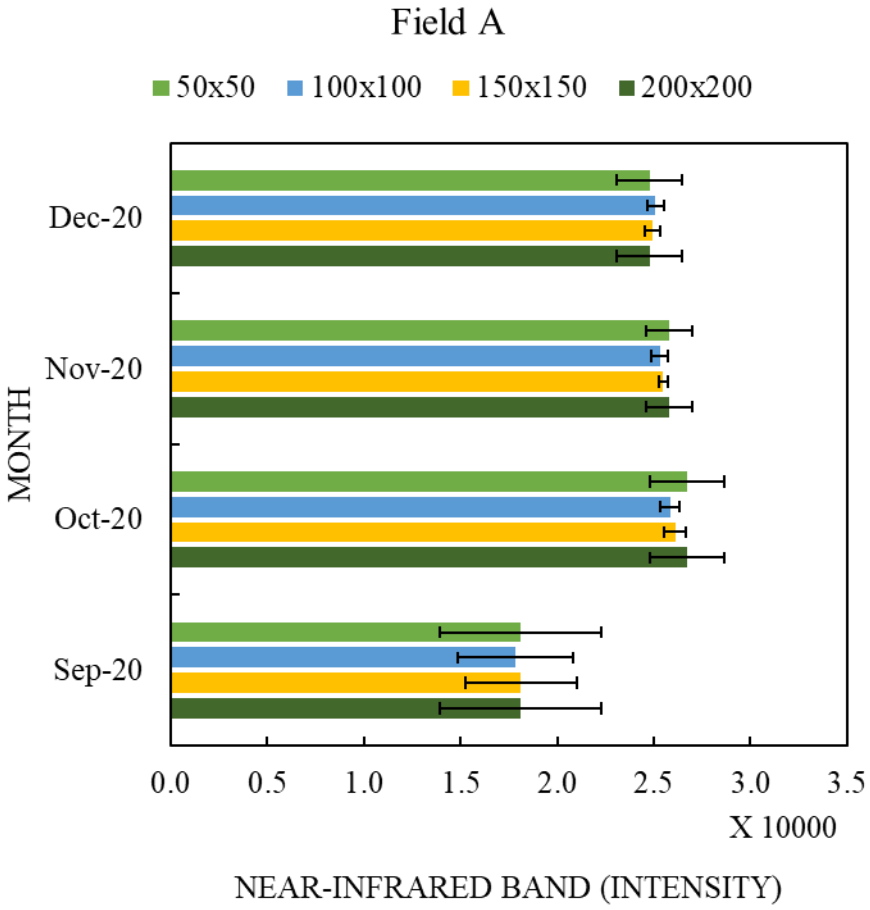

Figure 4.10: Bars of averaged NIR pixel values of each image cropped size displayed from September to December 2020 on field A

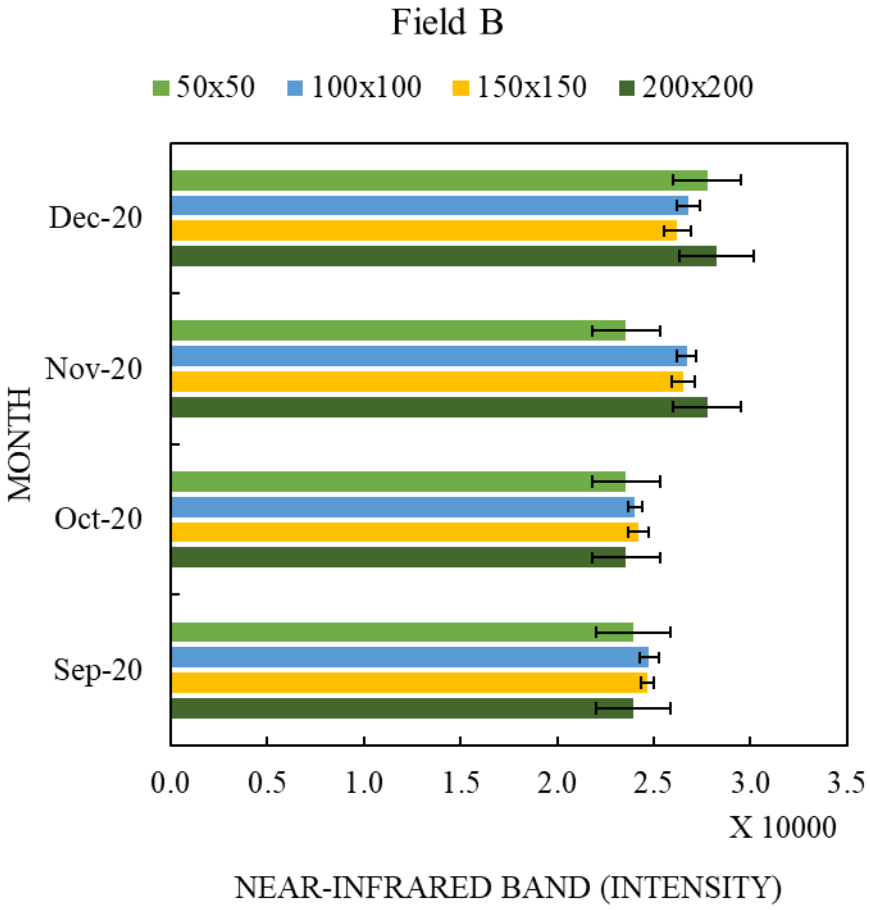

Figure 4.11: Bars of averaged NIR pixel values of each image cropped size displayed from September to December 2020 on field B

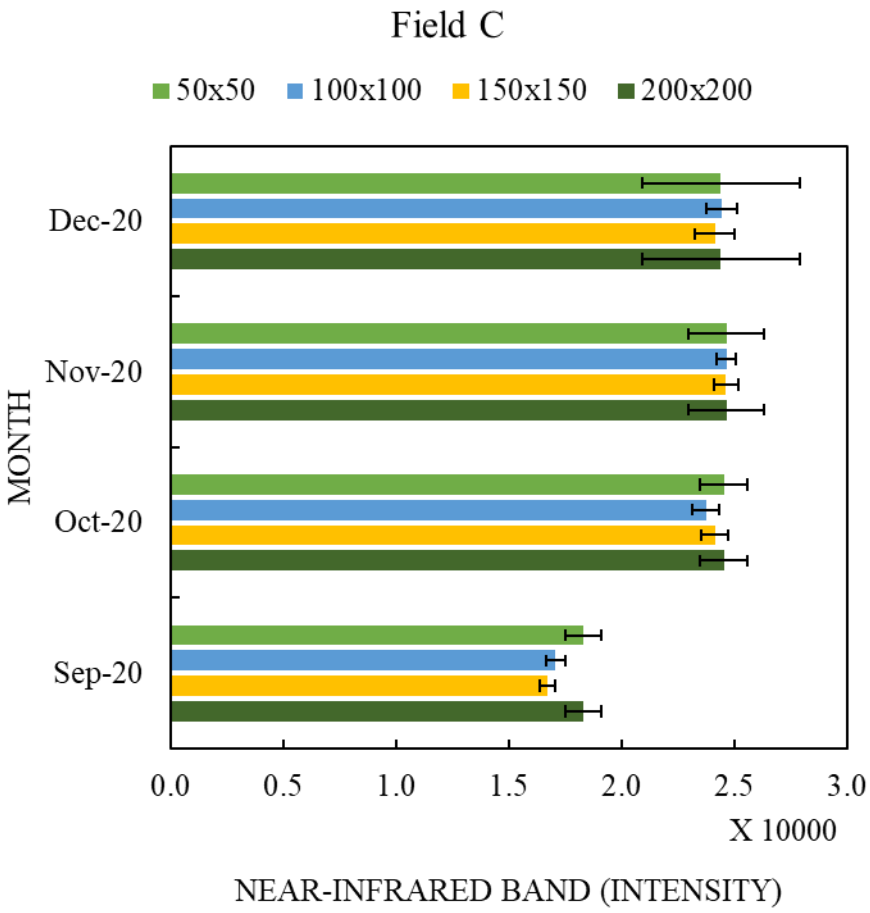

Figure 4.12: Bars of averaged NIR pixel values of each image cropped size displayed from September to December 2020 on field C

4.9 THE MONTHLY TREND OF VEGETATION INDICES

Figure 4.13 displays the monthly trends in NDVI for the three sugarcane fields. Fields B and C show similar NDVI trends, indicating that they might have experienced similar levels of damage from the tropical storm. In contrast, Field A exhibits steep increases in NDVI in October and slight increases in November, which may be attributed to the growth of new green sugarcane leaves. All fields demonstrate a decrease in NDVI in December, which can be linked to the onset of sugarcane senescence. Notably, the image size had a significant impact on the

observed NDVI trends. The 50×50 and 200×200 groups showed lower overall NDVI values than the 100×100 and 150×150 groups, reflecting the impact of image resolution on NDVI measurement. These findings underscore the importance of selecting an appropriate image size when analyzing NDVI trends.

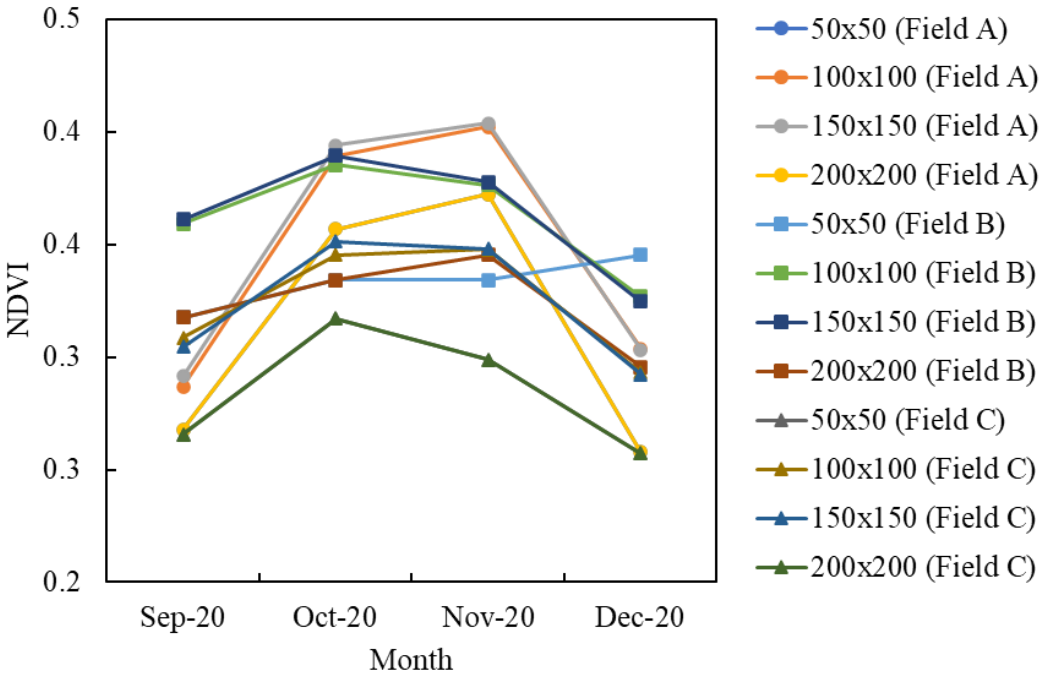

Figure 4.13: Monthly trends of NDVI

Figure 4.14 displays the monthly trends in $CI_{RedEdge}$ for the three sugarcane fields. Initially, $CI_{RedEdge}$ increased at different rates in October, as sugarcane leaves grew to recover from the stalk damage caused by the tropical cyclones. Field B and C both showed slight decreases in $CI_{RedEdge}$ from October to November, with the rate of decrease varying might depending on the extent of the damage and recovery energy in each field. Field A, which may have experienced lower levels of damage from the tropical cyclones than Fields B and C, exhibited an increase in $CI_{RedEdge}$

during October and November. In all three fields, a downward trend was observed in the last month due to the onset of sugarcane senescence. Notably, the image size had a significant impact on the observed $CI_{RedEdge}$ trends, with the data dividing into two distinct groups: the 50×50 and 200×200 group and the 100×100 and 150×150 group. These findings suggest that image size should be carefully considered when analyzing $CI_{RedEdge}$ trends.

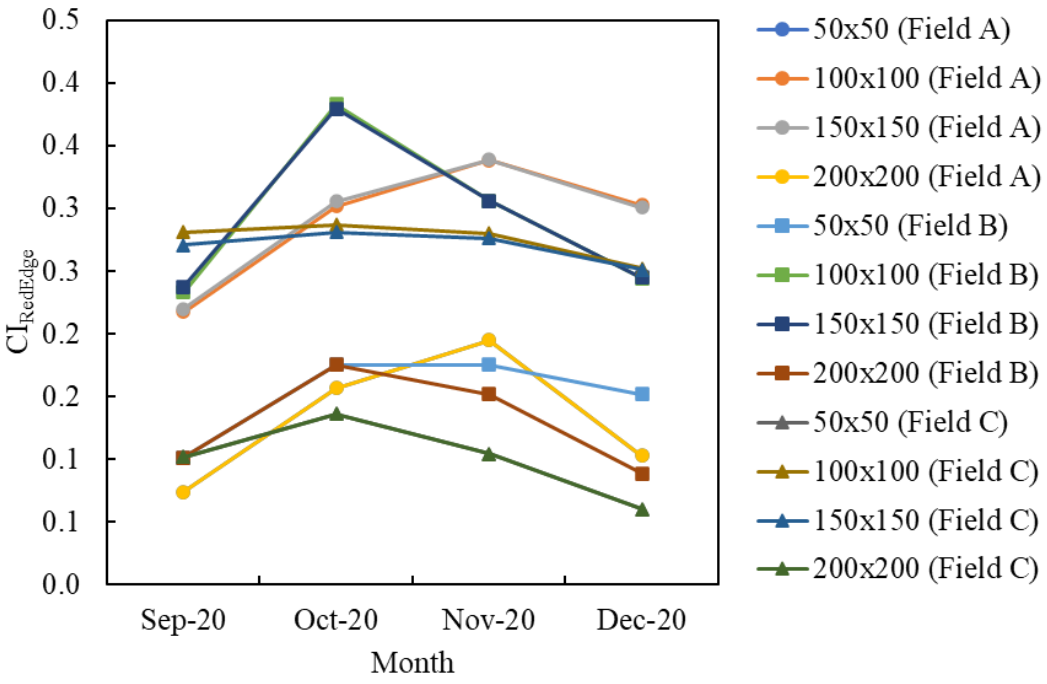

Figure 4.14: Monthly trends of $CI_{RedEdge}$

Figure 4.15 illustrates the monthly trend of $SRPI_b$ in the three sugarcane fields. Initially, most of the image sizes showed an increase in $SRPI_b$ values in October, followed by a mostly decreasing trend from October to November. The decline in $SRPI_b$ in October could be attributed to the sugarcane plants trading nitrogen in leaves to recover from the damage caused by the tropical cyclones. From October to November, the $SRPI_b$ values varied across the fields, likely reflecting differences in

the levels of damage and recovery energy. In the last months, a steep downward trend was observed across all sugarcane fields, as the plants fully recovered and started senescent. Notably, the data divided into two distinct groups based on image size: the 50×50 and 200×200 group and the 100×100 and 150×150 group. These findings suggest that image size should be carefully considered when analyzing $SRPI_b$ trends.

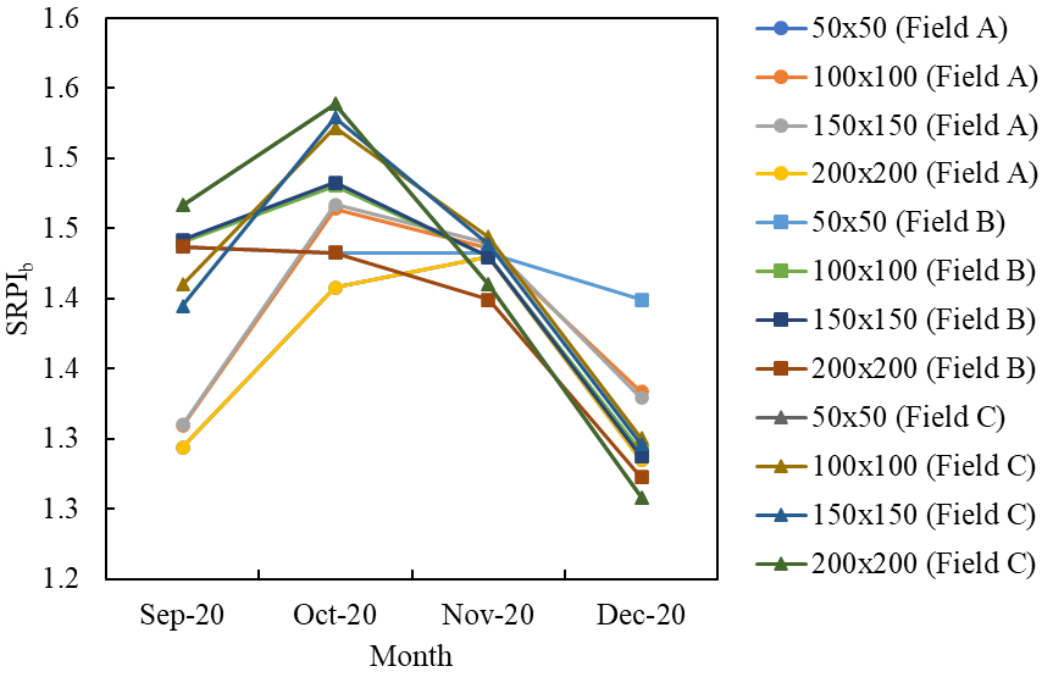

Figure 4.15: Monthly trends of $SRPI_b$

4.10 CORRELATION BETWEEN SUGAR QUALITY AND THREE VIS

The 12 SLR models were developed using Pol and three VIs (NDVI, $CI_{RedEdge}$, $SRPI_b$), as shown in Table 4.7. The accuracy of overall models (R^2) was 0.34 – 0.87. The $SRPI_b$ had correlations with Pol ($0.56 \leq R^2 \leq 0.87$), whereas $CI_{RedEdge}$ and NDVI shows a poor correlation with Pol ($0.34 \leq R^2 \leq 0.63$). Therefore, the best model for

Pol prediction is $SRPI_b$ of 150×150 image size model (R^2 = 0.87, RMSECV = 0.6%) since Pol in sugarcane might be directly or indirectly sensitive to nitrogen in sugarcane leaves.

The scatter plot in Figure 4.16 shows that sugarcane in October and November has the lowest Pol but highest $SRPI_b$ values in October and November due to damage from tropical storms. Conversely, the highest Pol and $SRPI_b$ values were observed in December, indicating that sugarcane had fully recovered and was producing more sugar. Furthermore, the difference in Pol or SRPI between September (Crystal marker) and October (Triangle marker) can be used to estimate the damage caused by the tropical storm. Finally, the y formula from the best correlation model was applied to develop a Pol map using $SRPI_b$ images, as shown in Figure 4.17.

Table 4-7: R^2, RMSEC, and RMSECV of simple linear regressions between averaged vegetation indices and Pol (n = 12)

Indicators	Image size	NDVI	$CI_{RedEdge}$	$SRPI_b$
R^2	50x50	0.34	0.40	0.56
RMSEC	50x50	1.3	1.3	1.1
R^2	100x100	0.61	0.39	0.86
RMSEC	100x100	1.0	1.3	0.6
R^2	150x150	0.63	0.39	0.87
RMSEC	150x150	1.0	1.3	0.6
R^2	200x200	0.53	0.55	0.62
RMSEC	200x200	1.1	1.1	1.00

R^2, coefficient of determination of calibration; RMSEC, root mean square error of cross-validation; SLR, simple linear regression.

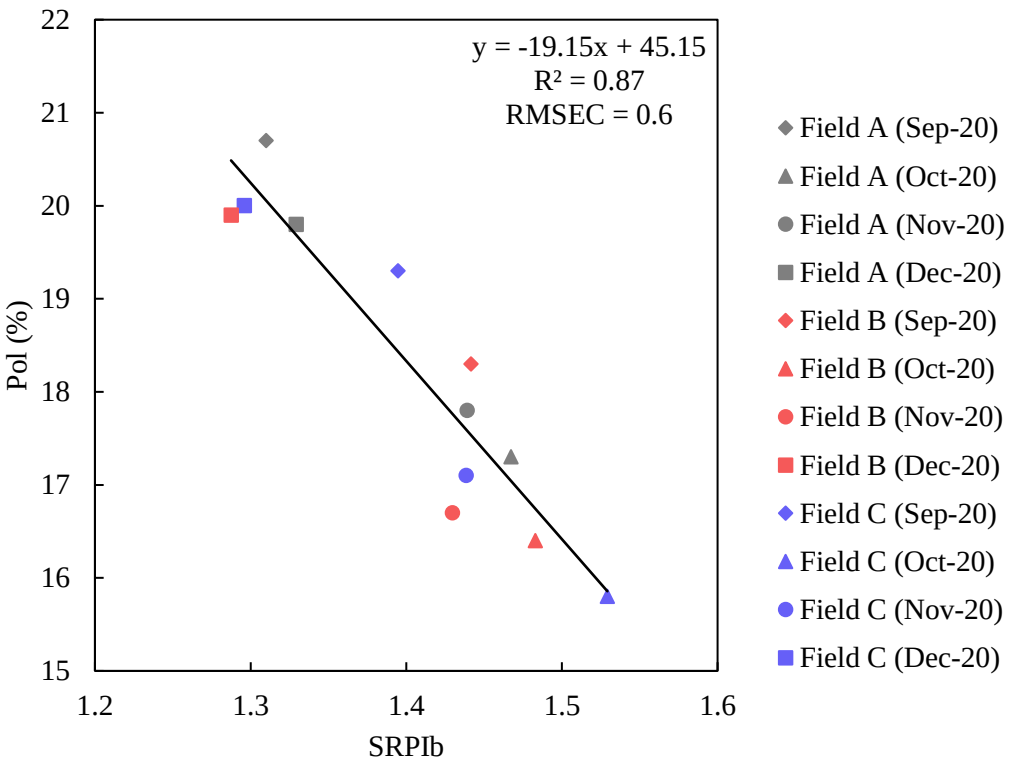

Figure 4.16: Correlation between Pol and $SRPI_b$ of 150×150 image size

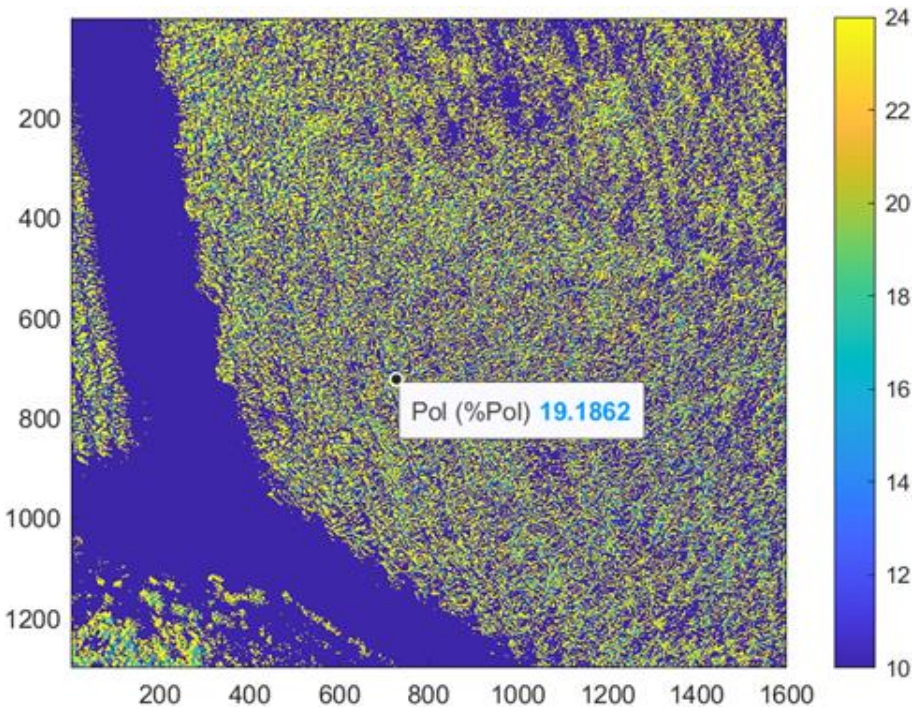

Figure 4.17: Example of Pol map

4.11 CORRELATION BETWEEN SUGAR QUALITY AND FIVE IMAGE BANDS

In Table 4-8, the 20 MLR models were developed using Pol and five image bands (R, G, B, RE, and NIR bands). The accuracy of overall models (R^2) was distributed within the range of 0.1–0.95 while most of the models could be used for Pol prediction except the 50×50 and 200×200 image size model because these models show low accuracy ($R^2_{CV} \leq 0.27$) while test by leave one out cross validation and the RMSECV of the model started to increase when using more than three factors. The MLR model shows that the first and second-best factors for Pol prediction were NIR and RE. Since these sugarcane reflectance canopy bands were near the wavelength ranges of chlorophyll content (approximately 680 nm)[10] and sugar content (approximately 910 nm)[11] which were keys to predicting sugar quality for a portable Vis-NIR spectrometer[2-4]. The best model for Pol prediction was the 150×150 image size model with five factors (R^2 = 0.95, RMSECV = 0.7%). In descending order, Pol was more affected by NIR, RE, G, R, and B bands. The R and B band combination was used to calculate $SRPI_{b,}$ which improves this MLR model accuracy according to the best SLR model showing $SRPI_b$ correlates to Pol.

Table 4-8: R^2 and RMSE of multiple linear regression models developed using the averaged value of image bands and Pol (n = 12)

Image Size (Pixels)	Factor (Band)					Indicators			
	1	2	3	4	5	R^2	RMSEC (%)	R^2_{cv}	RMSECV (%)
50 × 50	NIR					0.1	1.5	0	1.8
50 × 50	NIR	RE				0.32	1.3	0.1	1.7
50 × 50	NIR	RE	G			0.59	1	0.13	1.7
50 × 50	NIR	RE	G	B		0.6	1	0.1	1.8
50 × 50	NIR	RE	G	B	R	0.62	1	0.1	1.9
100 × 100	NIR					0.15	1.5	0	1.7
100 × 100	NIR	RE				0.63	1	0.49	1.1
100 × 100	NIR	RE	G			0.75	0.8	0.57	1.1
100 × 100	NIR	RE	G	R		0.85	0.6	0.67	0.9
100 × 100	NIR	RE	G	R	B	0.95	0.4	0.73	0.9
150 × 150	NIR					0.19	1.4	0	1.7
150 × 150	NIR	RE				0.64	1	0.5	1.1
150 × 150	NIR	RE	G			0.78	0.7	0.61	1
150 × 150	NIR	RE	G	R		0.88	0.6	0.72	0.9
150 × 150	NIR	RE	G	R	B	0.95	0.3	0.79	0.7
200 × 200	B					0.17	1.4	0	1.7
200 × 200	B	R				0.63	1	0.3	1.5
200 × 200	B	R	G			0.69	0.9	0.3	1.5
200 × 200	B	R	G	NIR		0.73	0.8	0.25	1.7
200 × 200	B	R	G	NIR	RE	0.82	0.7	0.27	1.7

Chapter 5: Concluding Remark

From measuring sugar quality and getting various data of sugarcane spectra and multispectral images to develop calibration models for predicting sugar quality in sugarcane. The results of the study can be summarized as follows.

5.1 CONCLUSION

The sugarcane industry plays a crucial role in many economies, and the quality of sugarcane is essential for efficient production. Traditionally, the sugar content in sugarcane is measured using the Pol and Brix tests, which require samples to be taken to a laboratory for analysis. This process can be time-consuming and costly, and there is a risk of errors during transportation and handling of the samples.

To address this issue, researchers have explored the use of portable spectrometers for in-field measurements of sugar quality. A benchtop Vis-NIR spectrometer can accurately measure sugar quality in sugarcane juice in a laboratory, and a portable Vis-NIR spectrometer can collect spectra from sugarcane stalks in the field and predict the sugar quality. While the portable spectrometer approach has shown promise, there are still factors that can affect the accuracy of the model, such as sugarcane wax, skin thickness, and skin diameter. Therefore, there is a need for further research to improve the accuracy of the prediction models.

In this context, the use of unmanned aerial systems (UAS) and multispectral cameras has also been explored to monitor sugarcane fields. The multispectral camera can collect image bands and calculate vegetation indices (VIs) such as NDVI, $CI_{RedEdge}$, and $SRPI_b$, which can be used for sugarcane field analysis. The results of a

study showed that in four different image sizes, cropped sugarcane canopy image bands and VIs correlated with Pol can be used to develop a Pol prediction model for UAS. However, the recommended image size is between 100×100 to 150×150 due to the spread out values in a 50×50 image size and the higher unwanted pixels in a 200×200 image size.

The $SRPI_b$ showed the best correlation with Pol, indicating that changes in nitrogen in sugarcane leaves might be directly or indirectly sensitive to the shift in Pol. Additionally, the combination of portable spectrometers and multispectral cameras shows the potential of smart agriculture, enabling quick and accurate measurement of the quality of sugarcane in the field. This can help farmers monitor the trend of Pol, estimate the health of sugarcane, and know the appropriate time for harvesting.

Overall, the use of portable Vis-NIR spectrometer and UAS technology has the potential to revolutionize the sugarcane industry, reducing costs and time associated with traditional laboratory testing, and enabling more efficient and accurate measurement of sugarcane quality in the field.

5.2 SUGGESTIONS

Various factors, including cultivar, weather, temperature, and soil type, can influence sugarcane stalk spectra and leaf canopy reflectance. However, chemical analysis is expensive, and multispectral images are affected by uncontrollable factors. Despite these challenges, it is possible to develop a robust calibration model for a portable Vis-NIR spectrometer and UAS through sufficient experimentation. To enhance the accuracy of sugarcane quality models, it is recommended to remove the sugarcane skin or wax before measuring the stalk spectra using a portable Vis-NIR

spectrometer. Additionally, developing a sugar quality database with different sugarcane varieties and conditions can improve the calibration model and enable it to be shared with other sugar mills could reduce the time to be succeed in developing model. Furthermore, implementing more sampling and analysis techniques for a portable Vis-NIR spectrometer and UAS can effectively minimize sample bias. Combining these instruments to address their weaknesses can lead to the development of sugar quality, sugarcane maturity, and health maps for UAS, which can provide valuable information to the industry and farmers for optimizing sugarcane production. By increasing efficiency and yield, such a system could greatly benefit both the sugar industry and farmers.

Bibliography

1. Poel PWvd, H. S and K. ST. *Sugar technology : beet and cane sugar manufacture*. Berlin: Verlag Dr Albert Bartens KG, 1998.

2. ICUMSA MB. The Determination of Pol (Polarisation), Brix and Fibre in Cane and Baggasse by the Wet Disintegrator Method - Official (Method GS5/7-1). Bartens, Berlin, Germany, 2007.

3. Roberts CA, Workman J, Reeves JB, et al. *Near-infrared Spectroscopy in Agriculture*. American Society of Agronomy, 2004.

4. Taira E, Ueno M, Furukawa N, et al. Networking system employing near infrared spectroscopy for sugarcane payment in Japan. *J near Infrared Spec* 2013; 21: 477-483. DOI: 10.1255/jnirs.1081.

5. Phuphaphud A, Saengprachatanarug K, Posom J, et al. Non-destructive and rapid measurement of sugar content in growing cane stalks for breeding programmes using visible-near infrared spectroscopy. *Biosystems Engineering* 2020; 197: 76-90. DOI: 10.1016/j.biosystemseng.2020.06.012.

6. Taira E, Ueno M, Saengprachatanarug K, et al. Direct Sugar Content Analysis for Whole Stalk Sugarcane Using a Portable near Infrared Instrument. *J near Infrared Spec* 2013; 21: 281-287. DOI: 10.1255/jnirs.1064.

7. Taira E, Ueno M, Takashi S, et al. Non-destructive quality measurement system for cane stalks using a portable NIR instrument. *Int Sugar J* 2015; 117: 430-433.

8. Amarasingam N, Ashan Salgadoe AS, Powell K, et al. A review of UAV platforms, sensors, and applications for monitoring of sugarcane crops. *Remote*

Sensing Applications: Society and Environment 2022; 26. DOI: 10.1016/j.rsase.2022.100712.

9. Xue JR and Su BF. Significant Remote Sensing Vegetation Indices: A Review of Developments and Applications. *Journal of Sensors* 2017; 2017: 1-17. DOI: Artn 1353691

10.1155/2017/1353691.

10. Peñuelas J, Gamon JA, Fredeen AL, et al. Reflectance indices associated with physiological changes in nitrogen- and water-limited sunflower leaves. *Remote Sensing of Environment* 1994; 48: 135-146. DOI: 10.1016/0034-4257(94)90136-8.

11. Chea C, Saengprachatanarug K, Posom J, et al. Sugar Yield Parameters and Fiber Prediction in Sugarcane Fields Using a Multispectral Camera Mounted on a Small Unmanned Aerial System (UAS). *Sugar Tech* 2020; 22: 605-621. DOI: 10.1007/s12355-020-00802-5.

12. Agriculture DoFaFOP. Sugar cane production situation of 2019 in Okinawa Prefecture (In Japanese). 2020, p. 64.

13. Takagi H, Sato M and Matsuoka M. *A Guidebook for Sugarcane in Japan*. Organizing Committee of the ISSCT Joint 12th Germplasm & Breeding and 9th Molecular Biology Workshops and Japanese Society of Sugar Cane Technologists (JSSCT), 2018, p.45.

14. Ricaud C, Egan BT, Gillaspie AG, et al. *Diseases of Sugarcane: Major Diseases*. 1st ed.: Elsevier Science, 1989, p.389.

15. Sivanesan A and Waller JM. *Sugar Cane Diseases (Phytopathological Papers)*. 1st ed.: CABI, 1986, p.88.

16. Sharma R and Tamta S. A review on red rot: The "Cancer" of sugarcane. *Journal of Plant Pathology and Microbiology S1 :003* 2015. DOI: 10.4172/2157-7471.S1-003.

17. Elsharif AA and Abu-naser SS. An Expert System for Diagnosing Sugarcane Diseases. *International Journal of Academic Engineering Research (IJAER)* 2019; 3: 19-27.

18. Khan A and Yadav MS. Image Processing Based Disease Detection for Sugarcane Leaves. *International Journal Of Advance Research, Ideas And Innovations In Technology* 2017; 3: 497-502.

19. Nithya K, Bukhari KAIM, Valluvaparidasan V, et al. Molecular detection of Colletotrichum falcatum causing red rot disease of sugarcane (Saccharum officinarum) using a SCAR marker. *Annals of Applied Biology* 2012; 160: 168-173. DOI: 10.1111/j.1744-7348.2011.00529.x.

20. Prefectural O. The annual report of sugarcane and sugar production results in Okinawa prefecture 2016/17 (In Japanese). In: Naha, 2017, pp.1-64.

21. Matsuoka M. Sugarcane cultivation and sugar industry in Japan. *Sugar Tech* 2018; 8: 3-9. DOI: 10.1007/bf02943734.

22. Shinzato Y, Uehara K and Ueno M. Adaptability of small-sized sugarcane harvesters in Okinawa. *Engineering in Agriculture, Environment and Food* 2015; 8: 207-211. DOI: 10.1016/j.eaef.2015.10.002.

23. Wienese A and Reid MJ. Soil in cane: its measurement, its effect on milling, and methods of removal. In: *Proc S Afr Sug Technol Ass* 1997, pp.130-134.

24. Tulip JR and Moore WE. Identification of trash in cane using machine vision. *Proc Aust Soc Sugar Cane Technol*. 2008, p. 464-476.

25. Phuphaphud A, Saengprachatanarug K, Posom J, et al. Effects of Waxy Types of a Sugarcane Stalk Surface on the Spectral Characteristics of Visible-Shortwave Near Infrared Measurement. *Engineering Journal* 2019; 23: 13-24. DOI: 10.4186/ej.2019.23.1.13.

26. Aparatana K, Naomasa Y, Sano M, et al. Predicting sugarcane quality using a portable visible near infrared spectrometer and a benchtop near infrared spectrometer. *J near Infrared Spec* 2022; 31: 14-23. DOI: 10.1177/09670335221136545.

27. Savitzky A and Golay MJE. Smoothing and Differentiation of Data by Simplified Least Squares Procedures. *Analytical Chemistry* 2002; 36: 1627-1639. DOI: 10.1021/ac60214a047.

28. Esbensen KH, Guyot D, Westad F, et al. *Multivariate Data Analysis: In Practice : an Introduction to Multivariate Data Analysis and Experimental Design*. CAMO, 2002.

29. Kennard RW and Stone LA. Computer Aided Design of Experiments. *Technometrics* 1969; 11: 137-148. DOI: 10.1080/00401706.1969.10490666.

30. Aparatana K, Ishikawa D, Maraphum K, et al. Non-destructive Laboratory Analysis of the Detection of Unhealthy Sugarcane Stalks Using a Portable Vis-NIR Spectrometer. *Engineering in Agriculture, Environment and Food* 2022; 15: 72-80. DOI: 10.37221/eaef.15.2_72.

31. Aparatana K, Saengprachatanarug K, Izumikawa Y, et al. Development of sugarcane and trash identification system in sugar production using hyperspectral imaging. *J near Infrared Spec* 2020; 28: 133-139. DOI: 10.1177/0967033520905369.

32. Maraphum K, Saengprachatanarug K, Aparatana K, et al. Spatial mapping of Brix and moisture content in sugarcane stalk using hyperspectral imaging. *J near Infrared Spec* 2020; 28: 167-174. DOI: 10.1177/0967033520905370.

33. Osborne BGFTHPTOBG. *Practical NIR spectroscopy with applications in food and beverage analysis*. Harlow, Essex, England; New York: Longman Scientific & Technical ; Wiley, 1993.

34. Golic M, Walsh K and Lawson P. Short-wavelength near-infrared spectra of sucrose, glucose, and fructose with respect to sugar concentration and temperature. *Appl Spectrosc* 2003; 57: 139-145. 2003/11/13. DOI: 10.1366/000370203321535033.